AD-A061 614 AIR FORCE INST OF TECH WRIGHT-PAT''ERSON AFB OHIO F/G 1/3
A STUDY OF AN OPEN-LOOP SYSTEM FOR DECOUPLING AIRSPEED AND FLIG--ETC(U)
MAR 77 R JOSLIN, H OHMIYA

UNCLASSIFIED AFIT-CI-79-57T NL

END
DATE FILMED
1-79
DDC

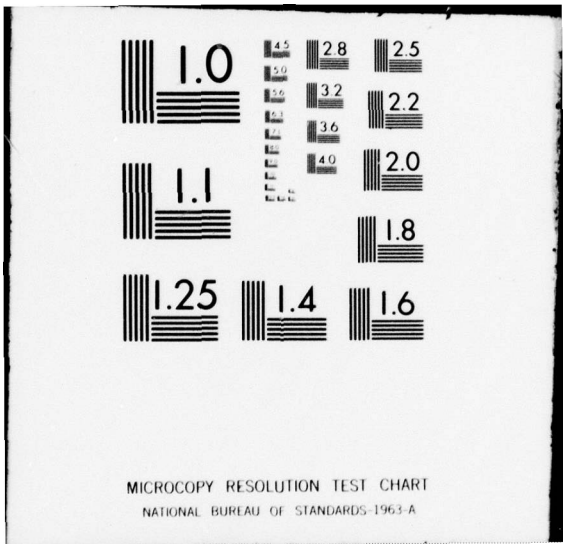
1.0
1.1
1.25
1.4
1.6
1.8
2.0
2.2
2.5
2.8
3.2
3.6
4.0
MICROCOPY RESOLUTION TEST CHART
NATIONAL BUREAU OF STANDARDS-1963-A

UNCLASSIFIED

SECURITY CLASSIFICATION OF THIS PAGE *(When Data Entered)*

REPORT DOCUMENTATION PAGE		READ INSTRUCTIONS BEFORE COMPLETING FORM
1. REPORT NUMBER CI 79-57T	2. GOVT ACCESSION NO.	3. RECIPIENT'S CATALOG NUMBER
4. TITLE *(and Subtitle)* A Study of an Open-Loop System for Decoupling Airspeed and Flight Path Angle Control		5. TYPE OF REPORT & PERIOD COVERED Thesis 6. PERFORMING ORG. REPORT NUMBER
7. AUTHOR(s) Randall Joslin and Hideaki Ohmiya		8. CONTRACT OR GRANT NUMBER(s)
9. PERFORMING ORGANIZATION NAME AND ADDRESS AFIT Students at Princeton University		10. PROGRAM ELEMENT, PROJECT, TASK AREA & WORK UNIT NUMBERS
11. CONTROLLING OFFICE NAME AND ADDRESS AFIT/CI WPAFB OH 45433		12. REPORT DATE 1977 13. NUMBER OF PAGES 60
14. MONITORING AGENCY NAME & ADDRESS *(if different from Controlling Office)*		15. SECURITY CLASS. *(of this report)* UNCLASSIFIED 15a. DECLASSIFICATION/DOWNGRADING SCHEDULE

16. DISTRIBUTION STATEMENT *(of this Report)*

Approved for Public Release, Distribution Unlimited

17. DISTRIBUTION STATEMENT *(of the abstract entered in Block 20, if different from Report)*

18. SUPPLEMENTARY NOTES

APPROVED FOR PUBLIC RELEASE AFR 190-17.

JOSEPH P. HIPPS, Major, USAF
Director of Information, AFIT

NOV 9 1978

19. KEY WORDS *(Continue on reverse side if necessary and identify by block number)*

20. ABSTRACT *(Continue on reverse side if necessary and identify by block number)*

DD FORM 1 JAN 73 1473 EDITION OF 1 NOV 65 IS OBSOLETE

UNCLASSIFIED

SECURITY CLASSIFICATION OF THIS PAGE *(When Data Entered)*

AD A061614

DDC FILE COPY

LEVEL II

D D C
RECEIVED
NOV 27 1978
E

79-57T

(6)

A STUDY OF AN OPEN-LOOP SYSTEM FOR DECOUPLING AIRSPEED AND FLIGHT PATH ANGLE CONTROL

by

(10) Randall Joslin
and
Hideaki Ohmiya

(9) Master's thesis

Department of Aerospace and Mechanical Sciences

(11) March 1977

(12) 80 p.

(14) AFIT-CI-79-57T

Submitted in partial fulfillment of the requirements for the Degree of Master of Science in Engineering from Princeton University

Prepared by:

Randall Joslin
Randall Joslin

Hideaki Ohmiya
Hideaki Ohmiya

Approved by:

Edward Seckel
Edward Seckel, Professor of
Aerospace and Mechanical Sciences

PRINCETON UNIVERSITY
Princeton, New Jersey

JOB

A Study of an Open-Loop System for Decoupling Airspeed and Flight Path Angle Control.

Randal J. Orlin & Hadeaki Ohmiya
Master of Science in Engineering - Princeton University.

ABSTRACT

Using an in-flight simulator, a simple longitudinal decoupling concept was compared with conventional airplane characteristics for the approach and landing tasks. The decoupling system allowed the pilot to command flight path angle changes with the stick with little or no accompanying speed change; likewise, speed changes with only small accompanying flight path changes could be made with throttle only. The unique feature of the concept is that it is an open loop (that is, non-feedback) control system. Results indicate that in calm air and up to moderate levels of turbulence the decoupling system provides a substantial reduction in pilot workload.
The program was supported by NASA, Langley Research Center, under Grant NSG 1234.

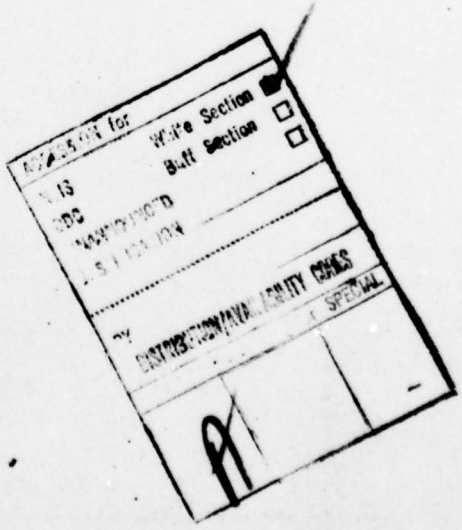

ACKNOWLEDGMENTS

This research was sponsored by the NASA, Langley Research Center. It was conducted by the Flight Research Laboratory of Princeton University under Grant NSG 1234. Mr. Harold Crane was the Technical Monitor for NASA. Professor Edward Seckel was the Principal Investigator at Princeton University.

The authors wish to express their sincere appreciation to Professor Edward Seckel for his guidance and suggestions during this project. The efforts of the two Princeton University evaluation pilots, Messrs. David R. Ellis and Walter B. Nixon, were also greatly appreciated. G. K. Olsen acted as safety pilot.

A special word of thanks goes to Messrs. Barton G. Reavis, Wilson M. McCredie, and Jeffrey G. Fitzwater for keeping the test airplane and equipment operational. The guidance of Mr. George E. Miller was also instrumental to the success of the program. The authors express their graditude to Professor Robert G. Joppa, visiting Professor from the University of Washington, for his guidance during the development of the Force-Feel Stick.

This tribute would not be complete without mentioning the special effort of Mrs. Nona Cloutier in typing this text.

The authors also wish to acknowledge the effort of each other and wish to thank their respective organizations (United States Air Force and Mitsubishi Heavy Industries Ltd., Japan) for having made the stay at Princeton possible.

This thesis carries number 1324-T in the records of the Department of Aerospace and Mechanical Sciences.

TABLE OF CONTENTS

		Page
	ABSTRACT	i
	ACKNOWLEDGEMENTS	ii
	TABLE OF CONTENTS	iii
	LIST OF FIGURES	v
	LIST OF TABLES	vii
SECTION 1.	INTRODUCTION	1
SECTION 2.	DESCRIPTION OF THE DECOUPLED SYSTEM	2
	Variables of Interest	2
	Requirements of the Decoupler	3
	Mathematical Development	5
	Flight Path Angle and Speed Commands	9
	Mechanizing the Decoupler	15
SECTION 3.	PILOT-AIRPLANE SYSTEM ANALYSIS	19
	Longitudinal Control	19
	Stick Washout Time Constant	22
	Comparison in Nominal Conditions	23
	Effects of Turbulence	24
	Effects of Off-Design Center of Gravity Position	31
	Decoupled Airplane with the One-Motor System	37
SECTION 4.	PRELIMINARY INVESTIGATION	39
	General Description	39
	Description of the Experiment	39
SECTION 5.	IN-FLIGHT SIMULATION	42
	In-Flight Simulator	42
	Flight Task and Evaluation Variables	44
	Test Variables	45
SECTION 6.	RESULTS AND DISCUSSION	47
	Flare and Touchdown with Decoupled Airplane	47
	Selection of Optimum Stick Washout Time Constant	47

		Page
SECTION 6.	RESULTS AND DISCUSSION (continued)	
	Comparative Evaluations in Nominal Conditions	48
	Effects of Flight in Turbulence	50
	Effects of Off-Design Center of Gravity	53
	Combined Effects of Turbulence and Center of Gravity Position	54
	Decoupled Airplane with One-Motor System	55
	Effects of Natural Airplane Coupling Parameters	55
	Implications and Recommendations	57
SECTION 7.	CONCLUSIONS	58
	REFERENCES	60
APPENDIX A.	FORCE-FEEL STICK SYSTEM	A1
APPENDIX B.	PILOT OPINION RATING SCALE	B1
APPENDIX C.	STABILITY DERIVATIVES OF BASIC NAVION	C1
APPENDIX D.	NOTATION	D1

LIST OF FIGURES

1. Time Histories of Basic Airplane Responses
2. Required Control for γ Decoupling
3. Numerator Singularities of Decoupled Airplane as a Function of S_T and τ_2
4. Decoupled System Block Diagram
5. Time Histories of Decoupled Response, Analog Simulation
6. Time Histories of Decoupled Response, In-Flight Results
7. Open Loop Stick and Throttle Transfer Functions; $j\omega$ Bode Magnitude Plots
8. Mechanization of Flight Path Controller
9. Mechanization of Speed Controller
10. Pole-Zero Locations of Speed Controllers
11. Comparison of Speed Response Characteristics
12. Time Histories of One-Motor System
13. Longitudinal Control Block Diagram of Decoupled Airplane
14. Longitudinal Control Block Diagram of Basic Airplane
15. Comparison of Stick Washout Time Constant; h/F_s root loci
16. Characteristics of Altitude Control for Piloted Decoupled Airplane
17. Characteristics of Altitude Control for Piloted Basic Airplane
18. Block Diagram of Pilot-Airplane System in Turbulence
19. Decoupled Airplane Altitude Control (h/h_c) Characteristics with S_T Variation
20. Decoupled Airplane Altitude Control with Pitch Attitude Inner Loop

21a. Time Histories of Decoupled Airplane; 10% Forward C.G.

b. Time Histories of Decoupled Airplane; 10% Aft C.G.

22. Locus of Poles and Zeros for γ Controller Varying M_α
23. γ/F_s Open Loop, Bode Characteristics; C.G. Variation
24. V/δ_{VC} Open Loop Bode Characteristics; C.G. Variation
25. Locus of Poles and Zeros for Speed Controller Varying M_α
26. Decoupled Airplane Altitude Control Characteristics with C.G. Variation

27. Closed Loop Altitude Control Bode Magnitude Diagram for Piloted Decoupled Airplane with C.G. Variation

28. Block Diagram Representation of the Ground Based Simulator

29. Effect of Washout Time Constant on Pilot Rating; Ground Based Simulation

30. Effect of C.G. Shift on Pilot Rating; Ground Based Simulation

31. Variable Response Navion In-Flight Simulator

32. Cockpit Interior of In-Flight Simulator

33. Flight Pattern

34. C.G. Shift Range for the Experiment

35. Navion Loading Weight — C.G. Envelope

36. Effect of Washout Time Constant on Pilot Rating; In-Flight Simulation

37. Flight Test Time Histories of the Decoupled and Basic Airplanes

38. Effects of Flight in Turbulence on Pilot Rating

39. Decoupled Airplane Time Histories of Flight in Turbulence

40. V/δ_{vc} Root Locus Sketches; τ_2 Variation

41. Effects of C.G. Shift on Pilot Rating

42. Combined Effects of Turbulence and C.G. Position on Pilot Rating

43. Time Histories of Decoupled Airplane Response with $M_{\delta t}$ Compensation

A1. Block Diagram Representation of Force Feel Stick System

A2. Second Order Stick Force Model

A3. Block Diagram Representation of Analog Computer System

B1. The Cooper-Harper Pilot Rating Scale

LIST OF TABLES

1. Response Characteristics of Flight Path Angle and Speed.

2. Pilot Ratings for Decoupled and Basic Airplane.

SECTION 1

INTRODUCTION

Most airplanes are "coupled" in the sense that for independent inputs of elevator, flap, or power, all of the flight variables — flight path angle, speed and pitch attitude — will generally exhibit transient and steady state changes; in order to have a response in one variable only (a "decoupled" response), the pilot would have to coordinate all three controls in a precise and continuous way. Generally the flap is not available for continuous controlling, in which case pure decouplung can't be achieved. However, by proper manipulation of the remaining controls — elevator and power — it is possible to change speed while holding a constant flight path angle, or change flight path at constant speed; pitch attitude is the variable which must change in both cases.

Although this manual coordination of two controls is obviously not beyond the capabilities of most people, experience with speed-holding autothrottles in transports has shown that partial decoupling can usefully simplify the piloting task during the landing approach. Also, most Navy carrier-based airplanes have an Approach Power Compensator System (APCS), a form of autothrottle which tends to seek a constant angle of attack; the pilot tracks the glidepath with stick inputs only.

Decoupling would be relatively easy to do in any modern airplane which has a fly-by-wire control system, extensive feedback of flight variables to the controls, and an air data computer. Such systems have been the subject of recent NASA studies (References 1, 2, and 3). General aviation aircraft operating today do not, however, have the systems referred to above, and this led to consideration of simplified open-loop methods of decoupling. The term open loop means that there is no feedback of flight variables to the various controls. This results in a simple system in terms of hardware, but complicated in the sense that it can be optimized for only one flight condition. By using already existing components in the aircraft, many of the benefits of decoupling can be realized without requiring high levels of sophistication. The methods suggested here would involve relatively little modification of the existing airplane.

This report presents an explanation of these methods and a description of ground based and in-flight simulation experiments. By means of the simulations, the general utility of the decoupled system was explored and compared with the basic aircraft. The optimization of the most important system parameter is explained as well as the affects of off-design center of gravity conditions and flight in turbulence.

SECTION 2

DESCRIPTION OF THE DECOUPLED SYSTEM

Variables of Interest

It is convenient here to consider longitudinal motion in terms of the variables, flight path angle (γ), pitch attitude (θ), and speed (V). Of the three, flight path angle and speed might be considered the more important for the approach and landing tasks; the following table summarizes the characteristics of the responses to movements of elevator (stick) and throttle.

Table 1. Response Characteristics of Flight Path Angle and Speed

CONTROL / FLIGHT VARIABLE	ELEVATOR	THROTTLE
FLIGHT PATH	High Frequency Transient Response; Steady State Response Depends on $d\gamma/dV$	Low to Medium Frequency Transient Response and Large Steady State Response
SPEED	Low to Medium Frequency Transient Response and Relatively Large Steady State Response	Medium Frequency Transient Response and no Steady * State Response

*This assumes no pitching moment due to thrust change.

Typical time histories of response to step inputs of elevator and throttle are shown in Figure 1 for a 70-kt approach condition. It is readily apparent that coordination of both controls would be required to change one variable without affecting the second variable.

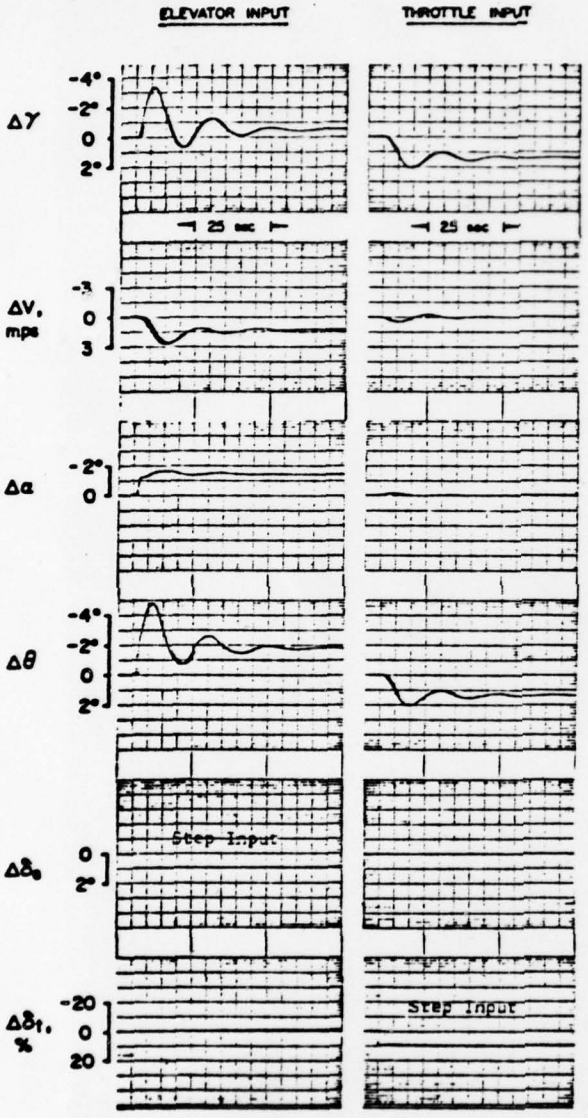

Figure 1. Time Histories of Basic Airplane Response

Requirements of the Decoupler

Since it is clearly possible for the pilot to manually coordinate stick and throttle to change either flight path or speed without affecting the other, then in principle it should be possible to interconnect these two controls to accomplish decoupling automatically and thus achieve a useful simplification of the piloting task.

The general design goals in the case of the flight path controller might be the following:

- Quick flight path response to control input
- Predictable steady state magnitude
- No unwanted transients (such as phugoid motions)

The first condition leads naturally to the choice of the stick (i.e., elevator) as the flight path controller, since for conventional airplanes flight path curvature can be initiated much more quickly with an angle of attack change than with a thrust change.

The speed control function falls to the throttle, and although quick, continuous controlling action might not be necessary, it would obviously be advantageous to have small flight path coupling and transient excitation for velocity commands.

Decoupled Flight Path Control - It is useful to consider the example of a pilot trying to manually change flight path angle without changing speed. The required control motions are of interest since they become a model for the decoupled controller. First, a step-like elevator input is applied to quickly curve flight path angle and establish an initial $\Delta\gamma$. Next, thrust must be increased to maintain speed, but at the same time the elevator must be returned to the trim position since the trim C_L is the same. If the pilot did not "washout" the elevator position he would find himself at a new speed as well as flight path angle. The power "washin" must be at the same rate as elevator washout and the amount added must be just enough to make $\Delta\gamma = \Delta\theta$ (since $\Delta\alpha$ = zero).

Time histories of the control motions required to get a smooth, quick change in γ (actually, a first-order exponential response) are shown in Figure 2. The amount of throttle due to stick (S_T) must be properly chosen for the particular configuration and flight condition so that the phugoid mode is not excited.

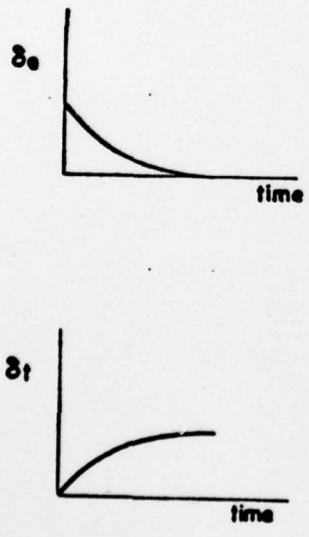

Figure 2. Required Control Motion for γ Decoupling.

Decoupled Speed Control - The speed controller uses the throttle to initiate a speed change and obtains the necessary steady state change in lift coefficient from a crossfeed to the elevator. If the proper amount of elevator is used, there will be no steady state flight path angle change. For a step throttle input the required elevator motion is a first-order lag; properly chosen τ_2 will be quite long (12 sec), and there will be little or no excitation of the phugoid mode.

Mathematical Development

The explanation of "Requirements of the decoupler" can also be developed mathematically using the linearized longitudinal equations of motion as shown below.

Assuming the decoupling of flight path angle and speed is accomplished, desirable output forms of flight path angle and speed with step input commands would seem to be first-order exponentials. A first-order response is desirable since the transient is smooth and the steady-state is predictable.

$$\gamma/\gamma_{command} = 1/(1 + \tau_1 s) \tag{1}$$

$$V/V_{command} = 1/(1 + \tau_2 s) \tag{2}$$

The required coordination of elevator (δ_e) and engine throttle in the decoupled system can be determined from the matrix of linearized longitudinal equations.

$$\begin{bmatrix} s+(D_V-T_V) & -(D_\alpha-g) & D_\alpha \\ L_V/V & -(s+L_\alpha/V) & L_\alpha/V \\ -M_V & M_{\dot{\alpha}}s+M_\alpha & s^2-(M_{\dot{\alpha}}+M_{\dot{\theta}})s-M_\alpha \end{bmatrix} \begin{bmatrix} \Delta V \\ \Delta\gamma \\ \Delta\theta \end{bmatrix} = \begin{bmatrix} T_{\delta t} & -D_{\delta e} \\ -L_{\delta t}/V & -L_{\delta e}/V \\ M_{\delta t} & M_{\delta e} \end{bmatrix} \begin{bmatrix} \Delta\delta_t \\ \Delta\delta_e \end{bmatrix} \tag{3}$$

The left-hand side of the equation forms the longitudinal characteristics which can be factored into the short period and phugoid modes. The right-hand side of the equation represents the inputs through the elevator and the engine throttle.

For simplicity it is assumed that the engine throttle affects only the drag equation, hence $L_{\delta t} = M_{\delta t} = 0$ and the elevator affects only the moment equation, $D_{\delta e} = L_{\delta e} = 0$. And also it is assumed $M_V = 0$.

Decoupled Flight Path Angle Control - The required coordination of elevator and throttle to obtain the desirable flight path response can be calculated from the longitudinal equations by setting $\Delta V = 0$.

$$\begin{bmatrix} -T_{\delta t} & 0 & D_\alpha \\ 0 & 0 & L_\alpha \\ 0 & -M_{\delta e} & s^2-(M_{\dot\alpha}+M_{\dot\theta})s-M_\alpha \end{bmatrix} \begin{bmatrix} \Delta\delta_t \\ \Delta\delta_e \\ \Delta\theta \end{bmatrix} = \begin{bmatrix} D_\alpha-g \\ s+L_\alpha/V \\ -M_{\dot\alpha}s-M_\alpha \end{bmatrix} \Delta\gamma$$

$$= \begin{bmatrix} D_\alpha-g \\ +L_\alpha/V \\ -M_{\dot\alpha} \; -M_\alpha \end{bmatrix} \frac{1}{1+\tau_1 s} \Delta\gamma_{command} \tag{4}$$

Then

$$\begin{cases} \delta_e = \dfrac{\Delta'_{sp}}{M_{\delta e}\, L_\alpha/V} \; \dfrac{s}{1+\tau_1 s} \Delta\gamma_{command} & (5) \\ \delta_t = \dfrac{D_\alpha \; s+(g/V)L_\alpha/D_\alpha}{T_{\delta t}\, L_\alpha/V} \; \dfrac{1}{1+\tau_1 s} \Delta\gamma_{command} & (6) \end{cases}$$

Where

$$\Delta'_{sp} = s^2 - \left[M_{\dot\alpha}+M_{\dot\theta}-(L_\alpha/V)\right]s - M_\alpha - (L_\alpha/V)M_{\dot\theta} \quad \text{(short period polynominal approximation)}$$

The frequency range of interest is $\omega \leq 2$ rad/sec. This is generally the bandwidth that pilots find satisfactory (References 4 and 5). Within this frequency range, the above equations yield:

$$\begin{cases} \delta_e \cong \dfrac{\omega'^2_{sp}}{M_{\delta e}\, L_\alpha/V} \; \dfrac{s}{1+\tau_1 s} \Delta\gamma_{command} & (7) \\ \delta_t \cong \dfrac{g}{T_{\delta t}} \; \dfrac{1}{1+\tau_1 s} \Delta\gamma_{command} & (8) \end{cases}$$

The above equations define the required movements of elevator (washout) and engine throttle (first-order lag) to accomplish the flight path angle decoupling with favorable response of flight path angle and no speed change.

The amount of throttle due to elevator (S_T) may be also obtained from the above equations and is

$$S_T = \frac{-M_{\delta e} g L_\alpha / V}{\omega'^2_{sp}\, T_{\delta T}} \tag{9}$$

$$\omega'^2_{sp} = -M_\alpha - M_{\dot\theta}(L_\alpha/V) \cong -M_\alpha \tag{10}$$

Decoupled Speed Control - In a similar way, the coordination of elevator and engine throttle which gives favorable speed response and no flight path change can be obtained from the longitudinal equations by setting $\Delta\gamma = 0$.

$$\begin{bmatrix} -T_{\delta t} & 0 & D_\alpha \\ 0 & 0 & L_\alpha/V \\ 0 & -M_{\delta e} & s^2-(M_{\dot\alpha}+M_{\dot\theta})s-M_\alpha \end{bmatrix} \begin{bmatrix} \Delta\delta_t \\ \Delta\delta_e \\ \Delta\theta \end{bmatrix} = \begin{bmatrix} -s-(D_V-T_V) \\ -L_V/V \\ 0 \end{bmatrix} \cdot \Delta V$$

$$= \begin{bmatrix} -s-(D_V-T_V) \\ -L_V/V \\ 0 \end{bmatrix} \frac{1}{1+\tau_2 s}\, \Delta V_{command} \tag{11}$$

Then

$$\begin{cases} \delta_e = -\dfrac{L_V \Delta''_{sp}}{M_{\delta e} L_\alpha} \dfrac{1}{1+\tau_2 s}\, \Delta V_{command} & (12) \\ \\ \delta_t = \dfrac{s+\lambda}{T_{\delta t}} \dfrac{1}{1+\tau_2 s}\, \Delta V_{command} & (13) \end{cases}$$

Where $\Delta''_{sp} = s^2-(M_{\dot\alpha}+M_{\dot\theta})s-M_\alpha$ (short period polynominal approximation)

$\lambda = D_V - D_\alpha(L_V/L_\alpha)$ (speed stability)

In the frequency range $\omega \leq 2$ rad/sec as mentioned before;

$$\begin{cases} \delta_e \cong -\dfrac{L_V \omega''^2_{sp}}{M_{\delta e} L_\alpha} \dfrac{1}{1+\tau_2 s}\, \Delta V_{command} & (14) \\ \\ \delta_t = \dfrac{s+\lambda}{T_{\delta t}} \dfrac{1}{1+\tau_2 s}\, \Delta V_{command} & (15) \end{cases}$$

In general aviation airplanes, the link from the cockpit controller to the engine throttle is generally a simple mechanical link. Therefore, $[(s+\lambda)/T_{\delta t}][1/(1+\tau_2 s)]$ should be constant from which $\tau_2 = 1/\lambda$ (long time constant) is derived. Then the above equations yield:

$$\begin{cases} \delta_e \cong -\dfrac{L_v \omega''^2_{sp}}{M_{\delta e} L_\alpha} \dfrac{1}{1+(1/\lambda)s} \Delta V_{command} & (16) \\ \delta_t = (\lambda/T_{\delta t}) \Delta V_{command} & (17) \end{cases}$$

The amount of elevator due to throttle (T_s) can be derived from the above equations and is;

$$T_s = -\frac{L_v \omega''^2_{sp} T_{\delta t}}{M_{\delta e} L_\alpha \lambda} \quad (18)$$

$$\omega''^2_{sp} = -M_\alpha \quad (19)$$

Functions of Decoupling Parameters - The functions of the four parameters for decoupling (τ_1, τ_2, S_T, T_s) may be explained as follows:

- τ_1, Time constant of first-order exponential response in flight path angle due to a step input command, and also elevator washout time constant.
- τ_2, Time constant of first-order exponential response in speed due to a step input command; an off-design value of τ_2 causes unwanted phugoid excitation in speed response.
- S_T, The amount of throttle due to elevator in flight path control; an off-design value of S_T causes unwanted phugoid excitation in flight path response.
- T_s, The amount of elevator due to throttle in speed control; an off-design value of T_s causes unwanted steady state flight path response.

Zero steady state error in speed response due to a step input command of flight path angle controller can be achieved solely by introducing elevator washout, hence none of the four decoupling parameters have any effect on the steady state error in speed response.

The elimination of unwanted phugoid excursions in flight path response for the flight path angle controller and the similar elimination of unwanted phugoid excursions in speed response for the speed controller can be explained as a "pole-zero cancellation." The phugoid poles are essentially cancelled by producing zeros close by. For example, in the case of a flight path command, (shown in the top left section of figure 3) the transfer function of the decoupled airplane has five poles and two zeros. The poles represent three modes the basic airplane short period and phugoid modes, and a first-order lag (time constant τ_1) mode. The position of the zeros in the s-plane is governed by the value of S_T. It can be seen that the nominal value of S_T, which is obtained from equation (9), results in a zero location (shown with a square) close to the phugoid poles (shown with a solid square); this minimizes the unwanted phugoid excitation in flight path response. The speed command case is shown in the bottom left section of Figure 3. The nominal value of τ_2 results in zeros being positioned close to the phugoid poles, which similarly minimizes the unwanted phugoid excitation in speed response.

The right-hand parts of Figure 3 show the zeros of speed response for the flight path controller and flight path angle response for the speed controller. In both cases the nominal values of S_T or τ_2 locate zeros on the origin. It should be noted that even if S_T or τ_2 are not set at nominal values in Figure 3, zero steady state error in speed response due to flight path command or zero steady state error in flight path angle response due to a speed command will be obtained, because one of the two zeros is always positioned at the origin in both cases, although it is not plotted in Figure 3.

Flight Path Angle and Speed Commands

The elevator "washout" required to accomplish the flight path angle decoupling due to a step input of flight path command causes a similar movement of the stick because of the mechanical link between stick and elevator, and, therefore it is not suitable to use stick position as a flight path angle command. Although several other possibilities might be suggested, the one selected for simulation here was to make <u>stick force</u> the flight path angle command. This could be achieved using an electric trim system as detailed in a later section.

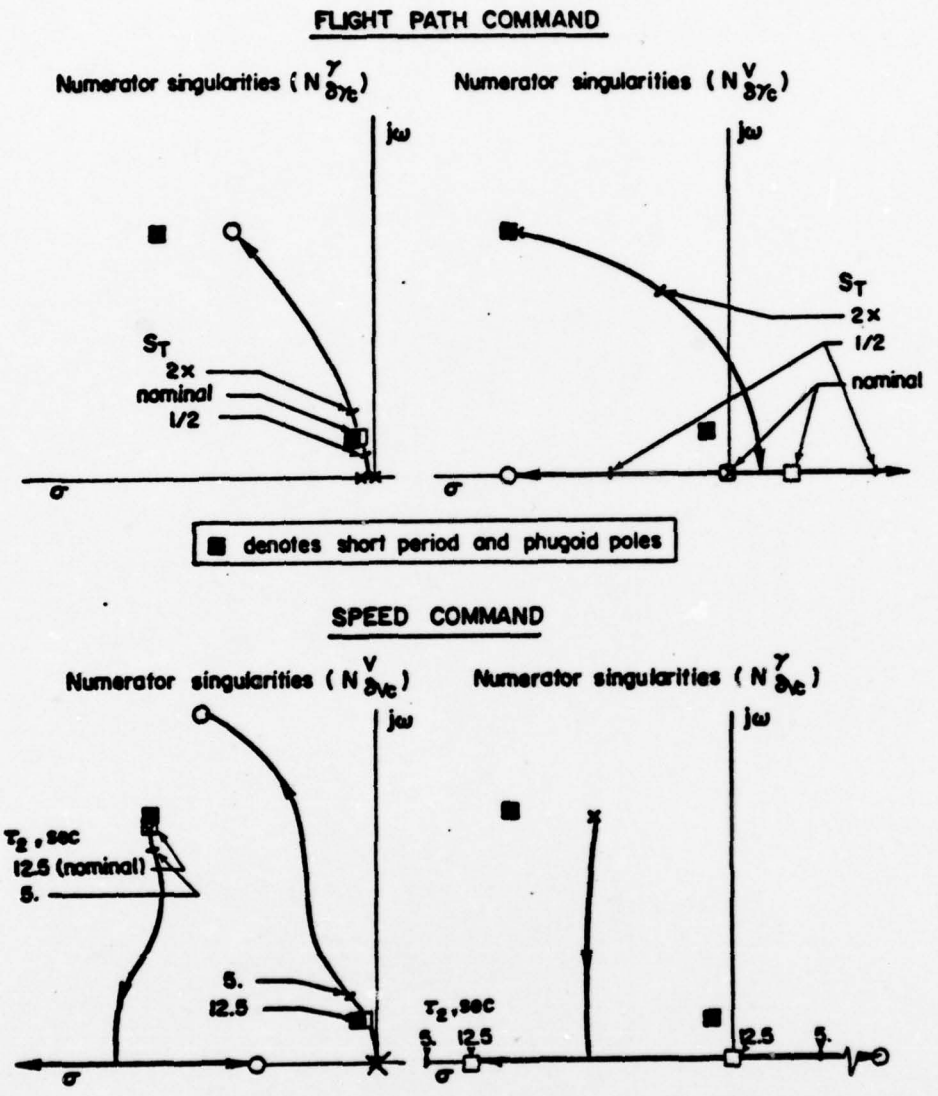

Figure 3. Transfer Function Numerator Singularities of Decoupled Airplane as a Function of S_T and τ_2.

Cockpit throttle position is suitable for use as the speed command. The matter of mechanizing the speed controller is a little more delicate than the flight path controller due to the possibility of interfering with the γ decoupler. This is also covered in a later section.

The conceptual block diagram of the decoupled system is shown in Figure 4.

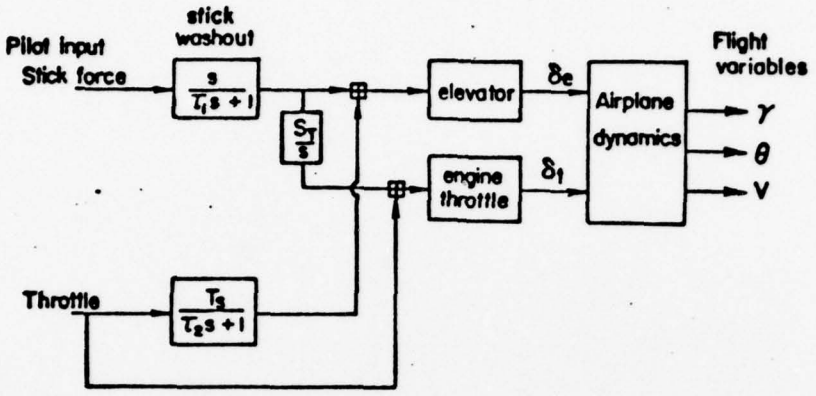

Figure 4. Decoupled System Block Diagram.

Figures 5 and 6 show time histories of analog computer and flight test results for a decoupled airplane using such an elevator washout system. The inputs were a step input of stick force for the flight path controller and a step input of throttle position for the speed controller. The motions of throttle and elevator due to the interconnects are shown.

The analog computer traces were obtained from an analog simulation of the Navion at an approach speed of 70 kt using the estimated stability derivatives of the Navion (Appendic C). The flight test results represent simulated approach conditions at altitude.

It can be seen in Figure 6 that elevator washes out beyond the initial trim position. This extra washout compensates for the pitching moment due to thrust variation ($M_{\delta t}$) which was assumed zero in the analog simulation.

Open loop Bode diagrams of the decoupled airplane (Figure 7) show the good characteristics of this system when compared to the basic airplane. In the case of the flight path angle controller, it can be seen that the open loop characteristics are flat out to about $\omega \cong .5$ rad/sec. Similarly the speed response to throttle input is flat at low frequencies implying it is possible to achieve steady state speed response, though the new steady state speed may be difficult to predict because of the long time constant.

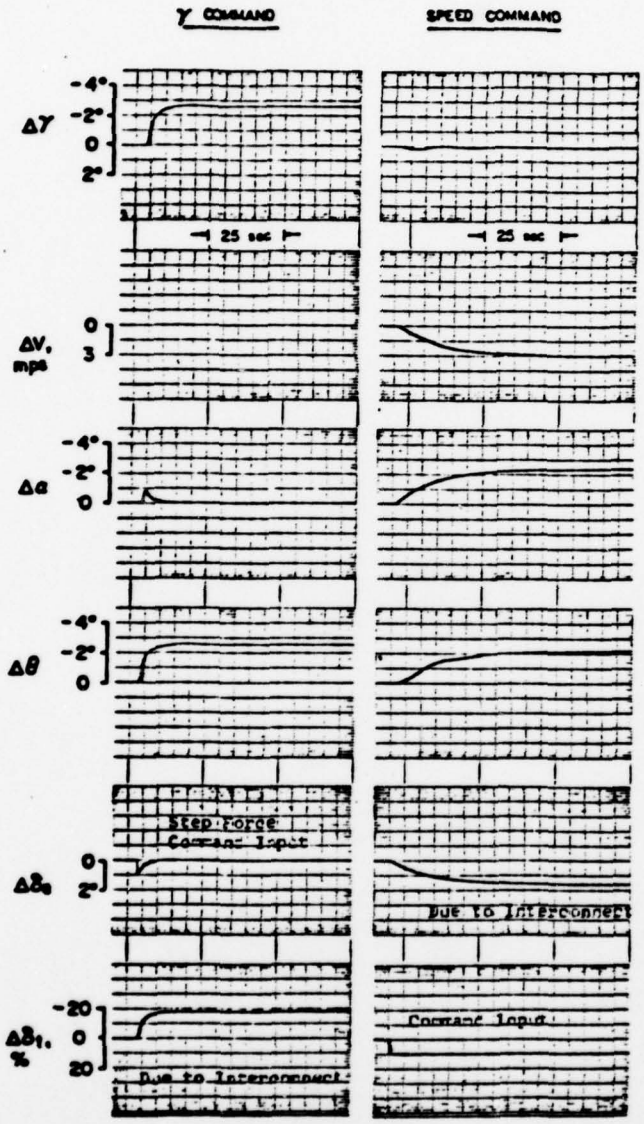

Figure 5. Time Histories of Decoupled Response, Analog Simulation.

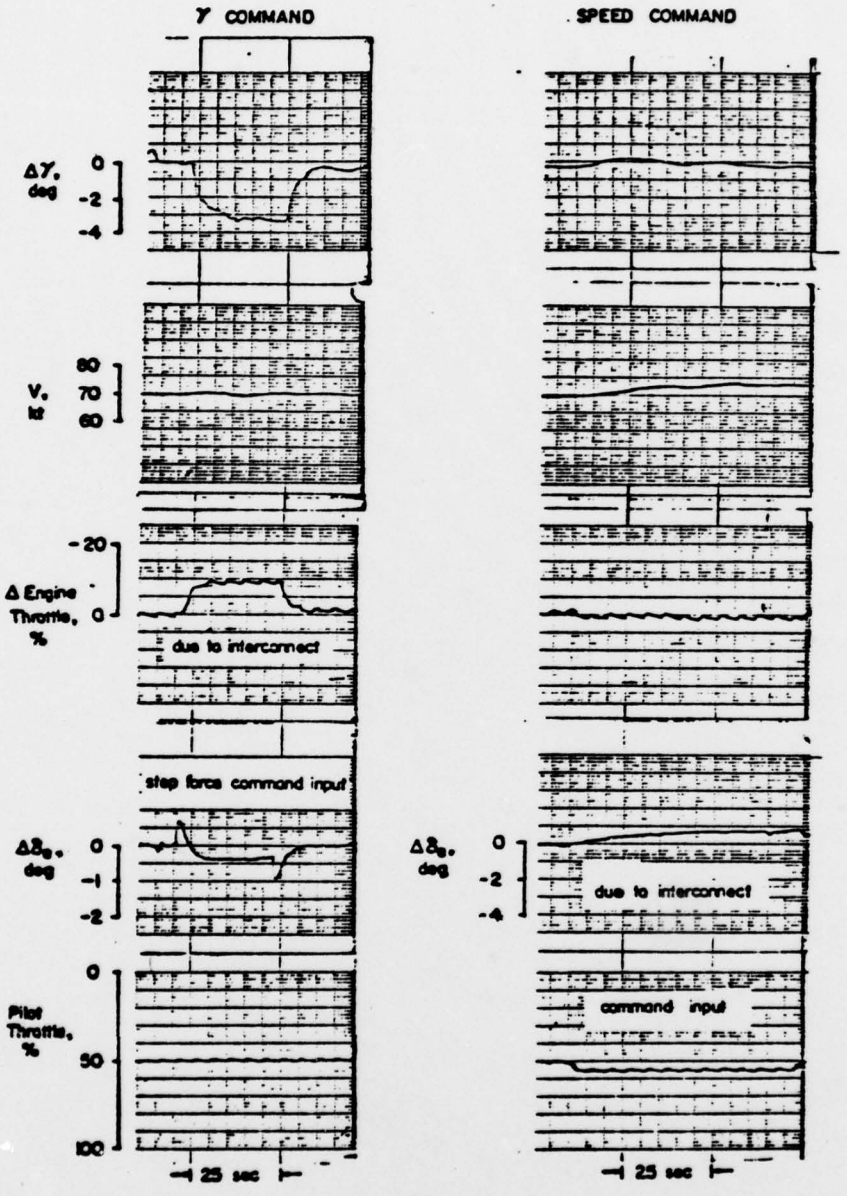

Figure 6. Time Histories of Decoupled Response, In-Flight Simulation

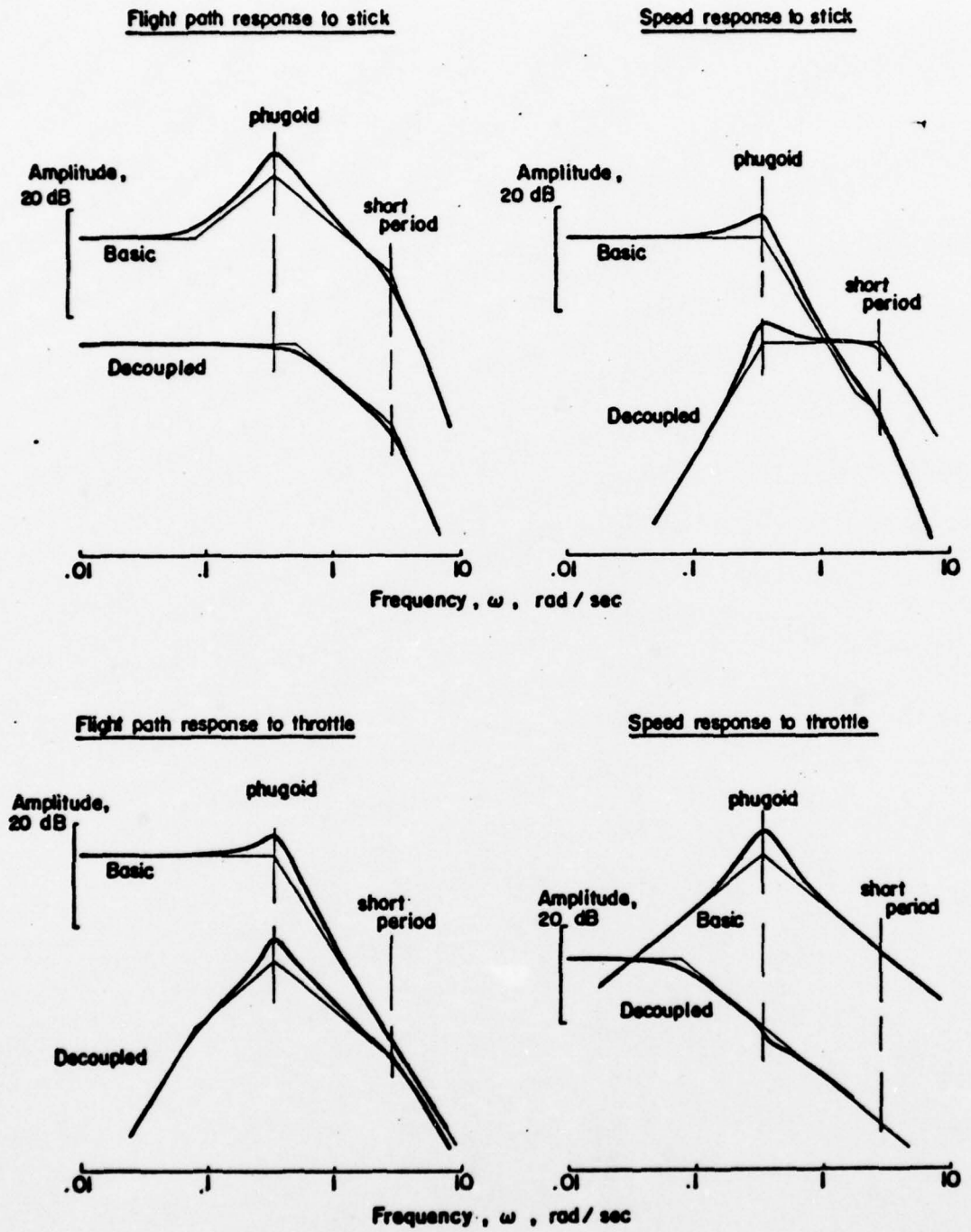

Figure 7. Open Loop Stick and Throttle Transfer Functions; jω Bode Magnitude Plots.

Mechanizing the Decoupler

Although several possible schemes for mechanizing the decoupler might be suggested, the one selected for simulation here was to make $\Delta\gamma$ proportional to stick force inputs. This could be accomplished by use of an electric trim system in the following manner (Figure 8). Elevator (or stick) deviation from the trim point is sensed and fed to the trim motor so that the resulting trim tab deflection creates a hinge moment tending to move the elevator back toward the trim position. As long as the stick is held away from the trim point the motor will continue to run, resulting in an increasing control force; on the other hand, if the pilot holds a constant force, he will find the stick "washing out" to the required position. The throttle is also connected to the trim motor in such a way as to "wash in" power in the required amount as the stick deflection is washing out.

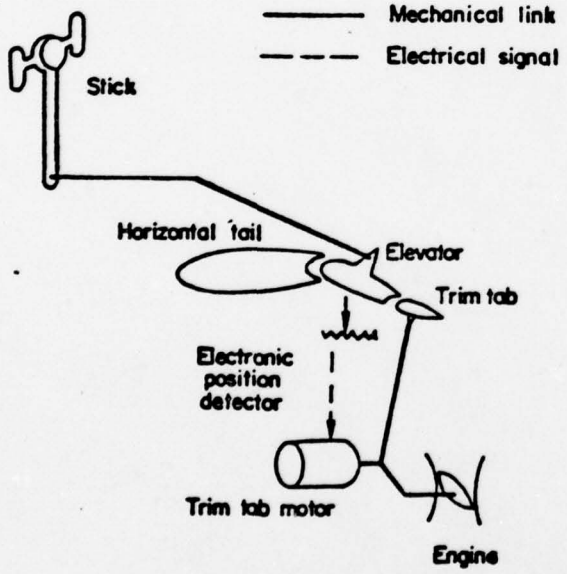

Figure 8. Mechanization of Flight Path Controller.

Retrimming to zero force to accommodate long-term flight path changes could be accomplished by means of a momentary disengage/reengage system or a mechanical tab override; another possibility is a separate trim tab motor.

Mechanizing the speed controller is a more delicate matter than the flight path case. The physical interconnect from throttle to elevator must be accomplished in a fashion that does not interfere with the stick washout. Two choices are possible here (Figure 9).

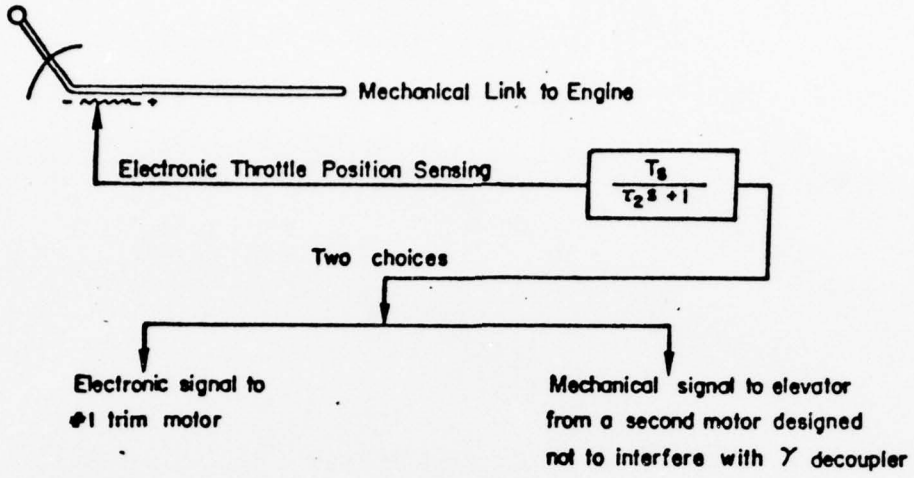

Figure 9. Mechanization of Speed Controller.

- a second motor could be installed to provide independent inputs to the elevator
- the original trim tab motor can be used realizing that there will now be some extra throttle activity due to the existing mechanical motor-throttle link required for γ-decoupling.

In the second case (one-motor system), the coupling of flight path angle due to speed controller input cannot be eliminated because of the extra throttle activity. Figure 10 shows the inadequate pole-zero cancellation in the one-motor system, resulting in some transient excitation. This is also evident in the open loop Bode magnitude diagram of Figure 11. Time histories for the response to a step input of throttle position are shown in Figure 12. Of particular interest is the extra throttle activity resulting in γ coupling; however, the speed response is essentially the same as for design system (Figure 5).

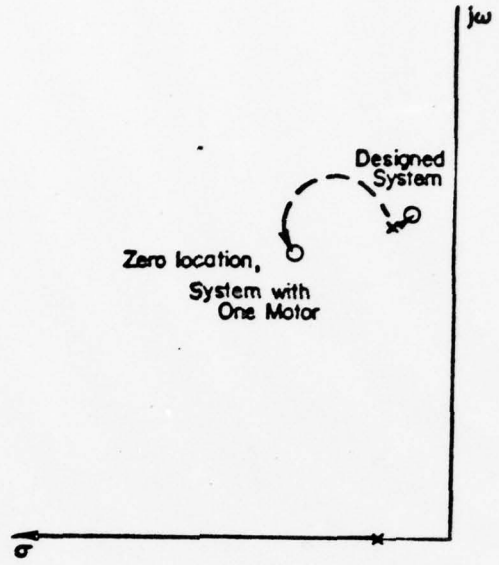

Figure 10. Pole-Zero Locations of Speed Controllers.

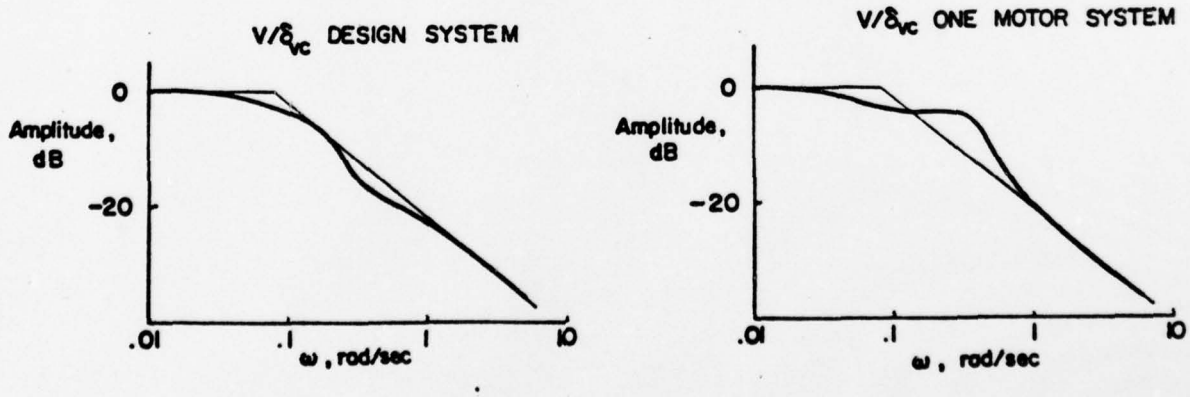

Figure 11. Comparison of Speed Response Characteristics.

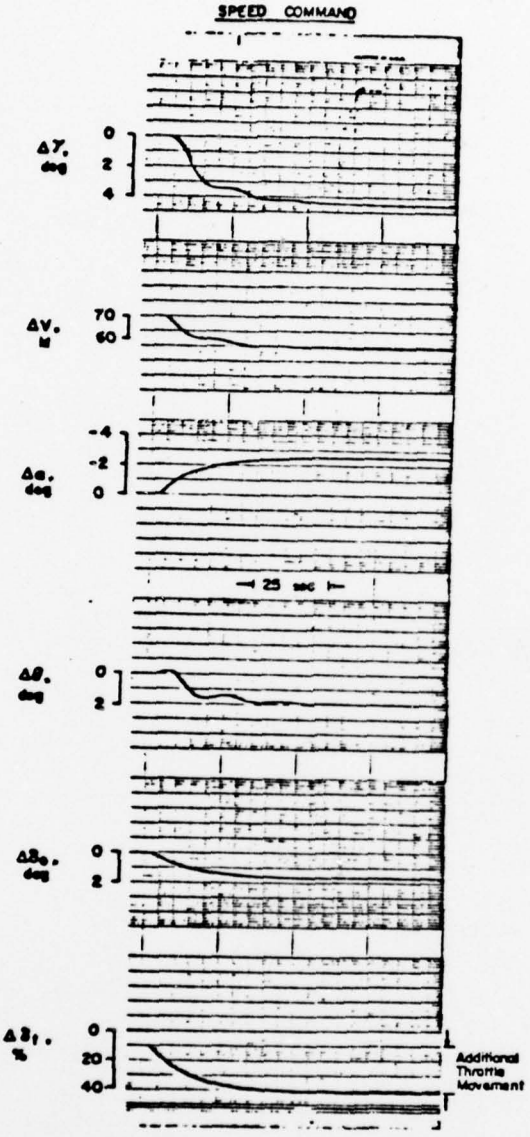

Figure 12. Time Histories of One-Motor System.

SECTION 3

PILOT-AIRPLANE SYSTEM ANALYSIS

The objective of the analytical study in this section is to predict the performance and pilot workload for the decoupled airplane when compared to the basic airplane in nominal conditions, and for off-design c.g. positions. The effects of flight in turbulence are also considered. The analysis will consider open-loop performance as well as performance with a pilot in the loop. Numerical values for Navion stability derivatives (Appendic C) were used for this analysis.

Longitudinal Control

Decoupled Airplane - Longitudinal control of the decoupled airplane during the approach may be examined in terms of the block diagram shown in Figure 13. Glideslope tracking can be accomplished by controlling altitude (glideslope deviation) with the flight path controller. Speed is similarly controlled by means of the speed controller. The pilot does not have to co-ordinate the two, since they are decoupled.

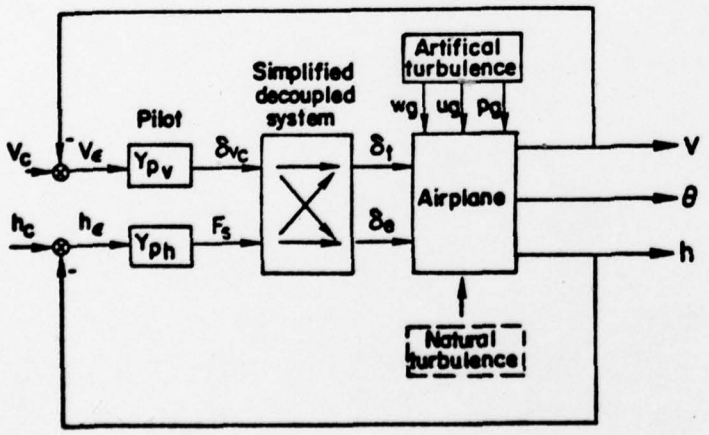

Figure 13. Longitudinal Control Block Diagram of Decoupled Airplane.

The response of the decoupled airplane to

turbulence disturbances will, of course, be altered by a pilot closing the loops, though neither altitude (or flight path angle) nor pitch attitude feedback to the decoupled stick can alter the basic airplane phugoid roots characteristics. This is detailed in a later portion of this section.

Basic Airplane - Longitudinal control of the basic airplane during the approach may be simplified and classified into two types represented by the block diagram shown in Figure 14.

Concerning Type I attitude control, there are of course, many other models that are possible. Type I control may not be the most favorable control but there are proponents of this method and particular cases that do use this kind of control may be cited. Reference 7 deals with many possible variations of decoupled control. One specific example is the so-called spoiler-Musketeer program (Reference 8). This airplane was configured such that throttle was the primary flight path control (altitude also) and the stick the airspeed control.

The major difference between these two types of control is that the pilot closes the altitude loop with throttle in Type I control and with stick (elevator) in Type II. In both types, a pitch attitude inner loop is closed with stick to compensate for the deficiencies in longitudinal dynamics which are generally poorly damped phugoid or short period modes. Pitch attitude feedback to stick (elevator) will help suppress pitch excursions excited by turbulence, but at the expense of higher pilot workload if the pilot is the element closing the θ loop. This will be discussed in much more detail in a later section.

The loop closure sequences of multiloop analysis in Type I control are first, pitch attitude to elevator, next, altitude to throttle, and finally speed to elevator in series with the pitch attitude loop. Similarly in Type II control, the sequences are first, pitch attitude to elevator, and altitude to elevator in series with the pitch attitude loop. Speed is controlled by feedback of speed to throttle. Speed closure is the last one in both types, since speed is considered as a secondary flight variable during the approach and is not continuously scanned and tightly closed by a pilot. Altitude (glideslope deviation) is the primary flight variable to be controlled, and therefore that loop is tightly closed.

Type I

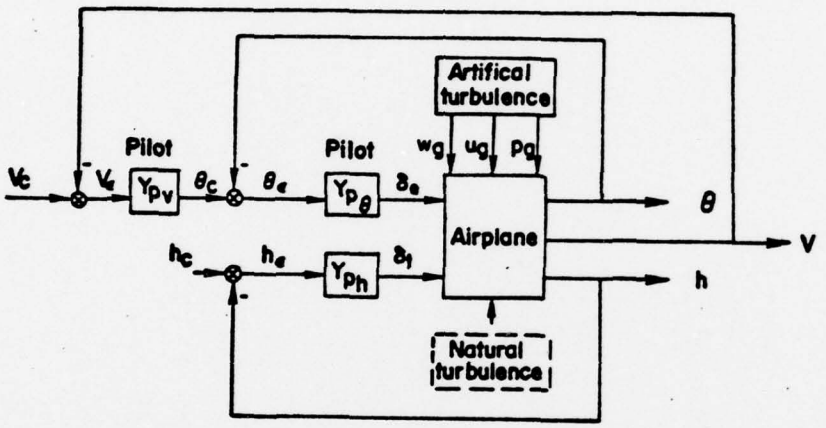

Type II

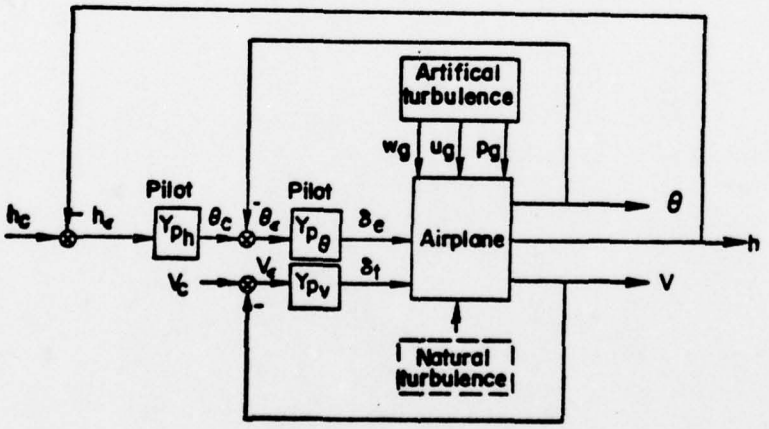

Figure 14. Longitudinal Control Block Diagram of Basic Airplane.

Stick Washout Time Constant

Before comparing the decoupled airplane with the basic airplane through the pilot-airplane system analysis, the effects of stick washout time constant τ_1 must be considered. Unlike the other three decoupling parameters (τ_2, S_T, T_s), τ_1 may be chosen freely since it does not effect the system decoupling as explained in the former section. The pilot-airplane system analysis of the altitude control shows that shorter time constants give larger closed loop bandwidths (Figure 15). Recent studies seem to support these findings concerning selection of τ_1. A study of the decoupled control system for a STOL transport indicated that increasing the level of L_α/V improves the bandwidth in the γ(or h) loop (Reference 3). Increasing the inverse time constant ($1/\tau_1$) in this case is essentially similar to increasing L_α/V. However, Reference 9 indicates that there may be limitations in how much $1/\tau_1$ may be increased. That study (which featured a control force washout)

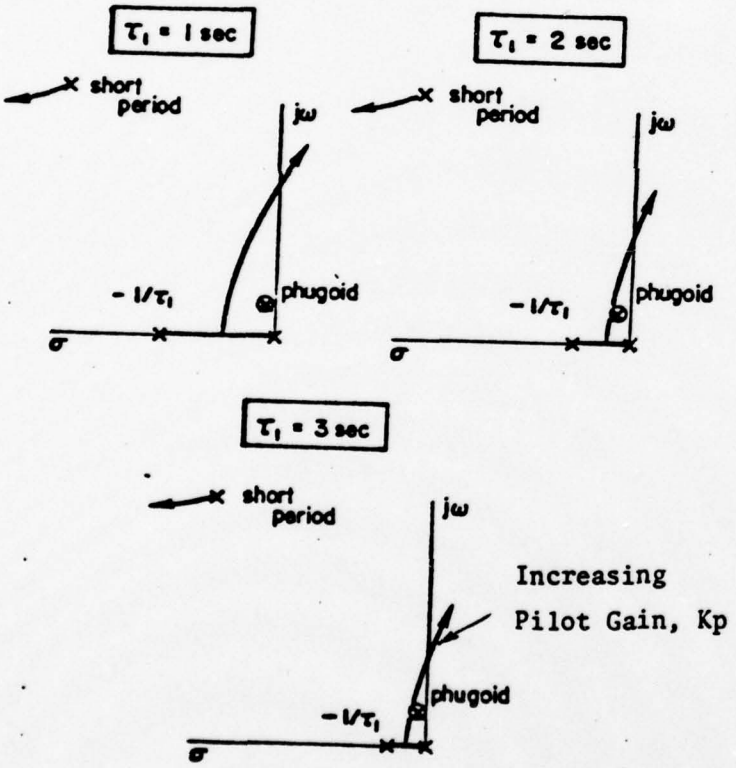

Figure 15. Comparison of Stick Washout Time Constant; h/F_s Root Loci.

indicated that increasing $1/\tau_1$ beyond $1/T_{\theta_2}$ ($\cong L_\alpha/V = 1.2$) would cause an overshoot in the response to a stick input. An additional constraint on τ_1 in this simple decoupled system is that despite promising bandwidth and response properties with short time constants, pilot opinion might be adversely affected by an obvious and fast stick motion.

Comparison in Nominal Conditions

Altitude control for the piloted decoupled airplane, and Types I and II piloted basic airplanes may be expressed by the following general transfer functions

$$\frac{h}{h_\epsilon} = \frac{Y_{ph} N^{\gamma}_{\delta\gamma c}}{s\,\Delta} \qquad \text{Decoupled airplane} \qquad (20)$$

$$\frac{h}{h_\epsilon} = \frac{Y_{ph}(N^{\gamma}_{\delta t} + Y_{p\theta} N^{\gamma}_{\delta t}\, {}^{\theta}_{\delta e})}{s(\Delta + Y_{p\theta} N^{\theta}_{\delta e})} \qquad \text{Basic airplane, Type I Control} \qquad (21)$$

$$\frac{h}{h_\epsilon} = \frac{Y_{ph} Y_{p\theta} N^{\gamma}_{\delta e}}{s(\Delta + Y_{p\theta} N^{\theta}_{\delta e})} \qquad \text{Basic airplane, Type II Control} \qquad (22)$$

using the format for multiloop equations described in Reference 10. For simplicity the pilot transfer function is assumed to be a simple gain and a 40 deg phase margin is chosen as the loop closure criterion. The frequency responses for altitude control of the piloted airplanes can be calculated and are shown in Figures 16 and 17 with the corresponding root loci. In the Bode magnitude diagrams "phugoid" or "short period" refer to basic airframe modes. It should be mentioned that the stick washout time constant for the decoupled airplane was set at 2 sec because this was found to be about the best value according to pilot opinion (shown in Section 5).

It can be seen that the Type II basic airplane has the largest bandwidth for altitude control and the Type I basic airplane has the smallest. From these figures, it is predicted that if the pilot adopts Type II basic airplane control, he may be able to perform the task of glideslope tracking

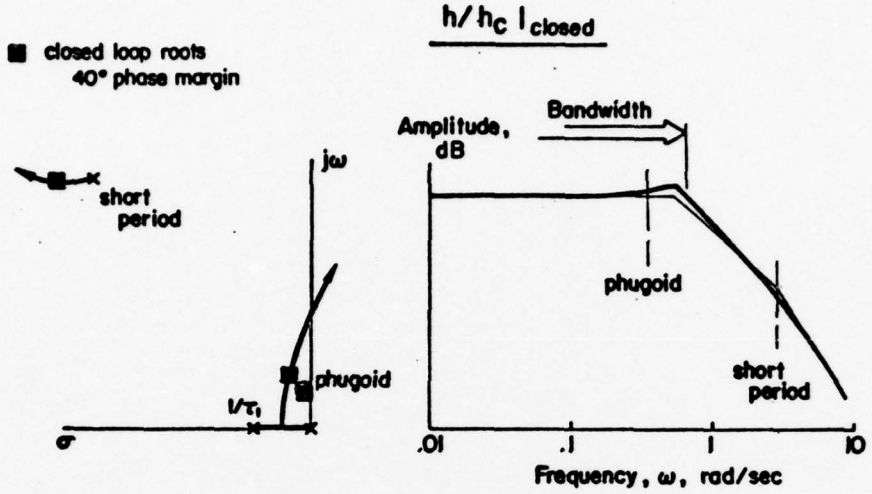

Figure 16. Characteristics of Altitude Control for Piloted Decoupled Airplane.

slightly better than if he was using decoupled controls; however, the pilot workload would increase since he would have to coordinate two controls.

The bandwidth of altitude control of the decoupled airplane is considered sufficient for the pilot to be able to perform the glideslope tracking task adequately. Altitude control with Type I basic control will suffer because of the smaller bandwidth and pilot workload will almost certainly increase because of the necessity for manipulating two controls.

Effects of Turbulence

The transfer functions for altitude response of the piloted airplane system due to turbulence disturbances, for example a fore-and-aft (u) gust, can be expressed as follows, neglecting pilot command inputs (Reference 11).

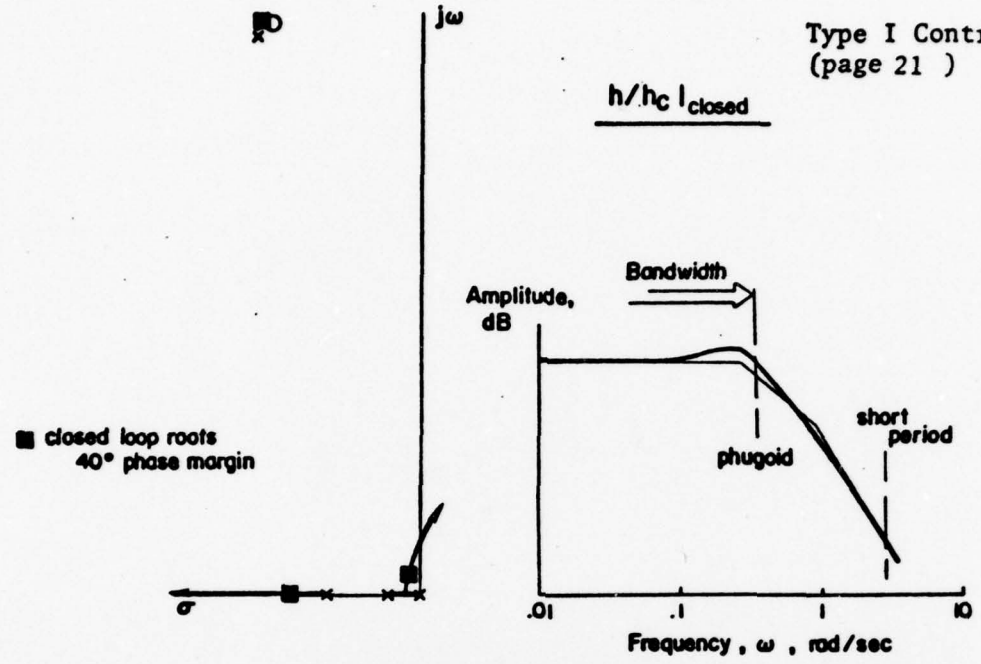

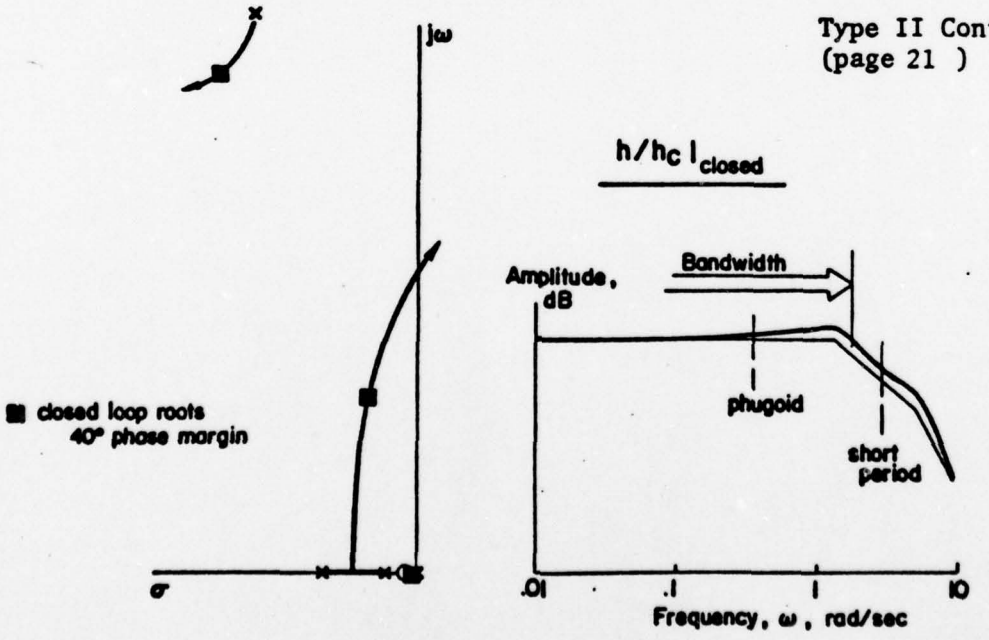

Figure 17. Characteristics of Altitude Control for Piloted Basic Airplane.

$$\frac{h}{u_g} = \frac{N_{u_g}^{\gamma}/s\Delta}{1+Y_{ph}(N_{\delta_{\gamma c}}^{\gamma}/s\Delta)} = \frac{N_{u_g}^{\gamma}}{s\Delta+Y_{ph}N_{\delta_{\gamma c}}^{\gamma}} \quad \text{Decoupled airplane} \qquad (23)$$

$$\frac{h}{u_g} = \frac{\dfrac{N_{u_g}^{\gamma}+Y_{p\theta}N_{u_g}^{\gamma}\,{}^{\theta}\delta e}{s(\Delta+Y_{p\theta}N_{\delta e}^{\theta})}}{1+\dfrac{Y_{ph}Y_{p\theta}N_{\delta e}^{\gamma}}{s(\Delta+Y_{p\theta}N_{\delta e}^{\theta})}} = \frac{N_{u_g}^{\gamma}+Y_{p\theta}N_{u_g}^{\gamma}\,{}^{\theta}\delta e}{s(\Delta+Y_{p\theta}N_{\delta e}^{\theta})+Y_{ph}Y_{p\theta}N_{\delta e}^{\gamma}} \quad \text{Basic airplane Type II} \qquad (24)$$

The denominators of the above equations represent the characteristics of the closed loop, pilot-airplane system and typical closed loop roots were shown in Figures 16 and 17.

In the decoupled airplane, the basic airframe phugoid mode will be excited by turbulence disturbances even with a pilot in the loop. If the altitude feedback loop has sufficient bandwidth, as shown in Figure 16, altitude excursions due to the excited phugoid mode should be suppressed, although speed excursions cannot be suppressed by the stick control.

If the speed excursions of the phugoid mode stay small it seems likely that the pilot will ignore them. Speed excursions will, however, become large enough to bother him in heavy levels of turbulence, and the pilot will start to use the throttle to suppress them. The additional throttle manipulation, however, will increase pilot workload.

On the other hand, for the basic airplane with a pilot closing an attitude loop, the phugoid mode of the basic airframe is altered. Excursions of flight path angle, pitch attitude or speed due to the turbulence disturbances might be smaller than in the case of decoupled airplane, which implies that the pilot may be able to better perform the task of tracking glide-slope. The pilot workload, however, when compared to the decoupled airplane is uncertain since he has to close an inner pitch attitude loop in addition to two outer loops (altitude and speed).

The above analysis suggests the possibility of the pilot closing a pitch attitude inner loop for the decoupled airplane similar to the basic airplane. By analyzing the open loop transfer function of stick to pitch attitude of the decoupled airplane, it becomes clear that phugoid poles are cancelled

by zeros close by, similar to the open loop transfer function of stick to flight path angle. This can be explained by the fact that pitch attitude response and flight path angle response are almost identical around the frequency of airplane phugoid mode. In ordinary airplanes, typical phugoid motion can be analyzed by assuming that angle of attack does not change during the motion. Therefore pitch attitude response and flight path angle response are the same since $\gamma = \theta - \alpha$.

It can be shown that a pitch attitude inner loop in the decoupled airplane cannot alter the phugoid characteristics, and the basic airframe phugoid mode will be excited due to turbulence disturbances. Thus the pitch attitude inner loop does not serve the same purpose — to move phugoid roots — as it does for the basic airplane.

The former explanation can be shown analytically as follows.

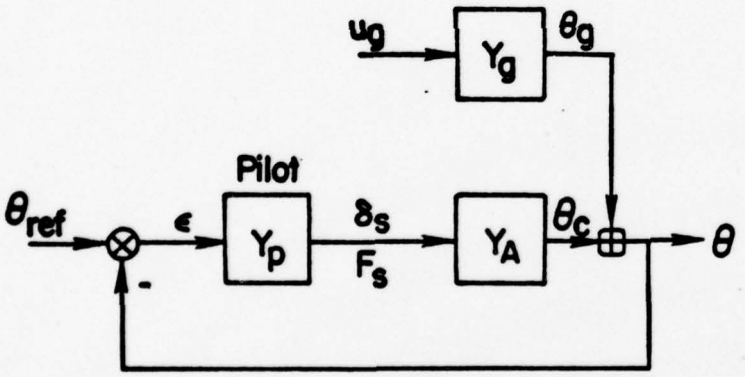

Figure 18. Block Diagram of Pilot-Airplane System in Turbulence.

Figure 18 shows in block diagram form how turbulence (for example, u_g gust) enters the pilot-airplane pitch attitude system. Assuming no pilot command input, the following relations are derived from the block diagram.

$$\theta = \theta_c + \theta_g = Y_G \cdot u_g + Y_p Y_A \cdot \epsilon \quad (25)$$

since $\epsilon = -\theta$, the above equation will yield

$$\frac{\theta}{u_g} = \frac{Y_G}{1 + Y_p Y_A} \quad (26)$$

For the basic airplane, the gust to pitch attitude transfer function Y_G and the pilot command to pitch attitude transfer function, Y_A, are represented by

$$Y_G = N^{\theta}_{u_g}/\Delta \tag{27}$$

$$Y_A = N^{\theta}_{\delta s}/\Delta \tag{28}$$

Substituting equations (27) and (28) into equation (26), the pitch attitude response of the piloted basic airplane due to the u_g gust disturbances can be expressed by

$$\left.\frac{\theta}{u_g}\right|_{\text{Basic}} = \frac{\frac{N^{\theta}_{u_g}}{\Delta}}{1+Y_p\cdot\frac{N^{\theta}_{\delta s}}{\Delta}} = \frac{N^{\theta}_{u_g}}{\Delta+Y_p\cdot N^{\theta}_{\delta s}}$$

$$= \frac{N^{\theta}_{u_g}}{(s^2+2\zeta\omega s+\omega^2)_{sp}(s^2+2\zeta\omega s+\omega^2)_{ph}+Y_pA_{\theta}\left[s+(1/T_{\theta_1})\right]\left[s+(1/T_{\theta_2})\right]} \tag{29}$$

where ph = phugoid

sp = short period .

The denominator represents the closed loop roots of the pitch attitude to elevator transfer functions, which contains a modified phugoid mode. For the decoupled airplane, Y_G is the same as for the basic airplane (equation 27). Y_A is

$$Y_A = N^{\theta}_{F_s}/(s+1/\tau_1)\Delta \tag{30}$$

where $N^{\theta}_{F_s} = A_{\theta}(s+1/T'_{\theta_2})(s^2+2\zeta\omega s+\omega^2)_{ph}$ and $T'_{\theta_2}\cong T_{\theta_2}$. Therefore equation (30) yields

$$Y_A = \frac{A_{\theta}(s+1/T'_{\theta_2})}{(s+1/\tau_1)(s^2+2\zeta\omega+\omega^2)_{sp}} \tag{31}$$

By substituting equation (27) and (31) into equation (26)

$$\left.\frac{\theta}{u_g}\right|_{\text{Decoupled}} = \frac{N^{\theta}_{u_g}}{1+Y_p\frac{A_{\theta}(s+1/T'_{\theta_2})}{(s+1/\tau_1)(s^2+2\zeta\omega s+\omega^2)_{sp}}}$$

$$= \frac{N^{\theta}_{u_g}}{\left[(s+1/\tau_1)(s^2+2\zeta\omega s+\omega^2)_{sp}+Y_pA_{\theta}(s+1/T'_{\theta_2})\right](s^2+2\zeta\omega s+\omega^2)_{ph}} \tag{32}$$

It can be seen that there is a phugoid mode in the closed loop response to gust disturbances.

The above analysis is equally valid for γ (or h), and also w_g. It demonstrates that θ and γ components of phugoid motion exist in the closed loop due to gust inputs. This does not imply, however, that they cannot be controlled. Pilots can operate on θ and γ excursions and suppress deviations if there is sufficient bandwidth in the closed loop response.

Recoupling of the Decoupled Airplane - Based on the decoupled airplane analysis with a pilot in the loop, there may be a possibility of altering the basic airframe phugoid response characteristics due to turbulence disturbances by changing S_T (stick to throttle crossfeed). This could be called recoupling of the decoupled system, since it is an off-design condition, which causes unwanted phugoid excitation due to flight path controller inputs. Steady state decoupling can still be achieved as explained in Section 2.

From the root locus analysis of altitude control shown in Figure 19, it can be seen that the modified phugoid mode of the piloted airplane can be changed to a more heavily damped and higher frequency mode by setting S_T at half of the nominal value. On the contrary, doubling the value of S_T results in a modified phugoid mode that is very lightly damped or even unstable.

If S_T is set at a value less than 0.5, the open loop stick to flight path angle response will have a noticeable transient response which might be annoying to the pilot.

Pitch Attitude Cue in Controlling Altitude with Decoupled Airplane - It appears possible that by scanning the pitch attitude indicator the pilot may obtain flight path angle information. A γ cue is usually difficult for the pilot to detect since the glideslope indicator used in an IFR approach actually shows the altitude deviation from the imaginary ideal glideslope. Of course, the pilot may be able to get flight path angle information from the rate of climb indicator, particularly if it is of the instantaneous (IVSI) type.

The analytical study of the decoupled airplane root locus (Figure 20) with a loop closure sequence similar to the Type II basic airplane control (θ inner, h outer) shows considerable improvement of the altitude control bandwidth. The bandwidth appears to be slightly larger than Type II control.

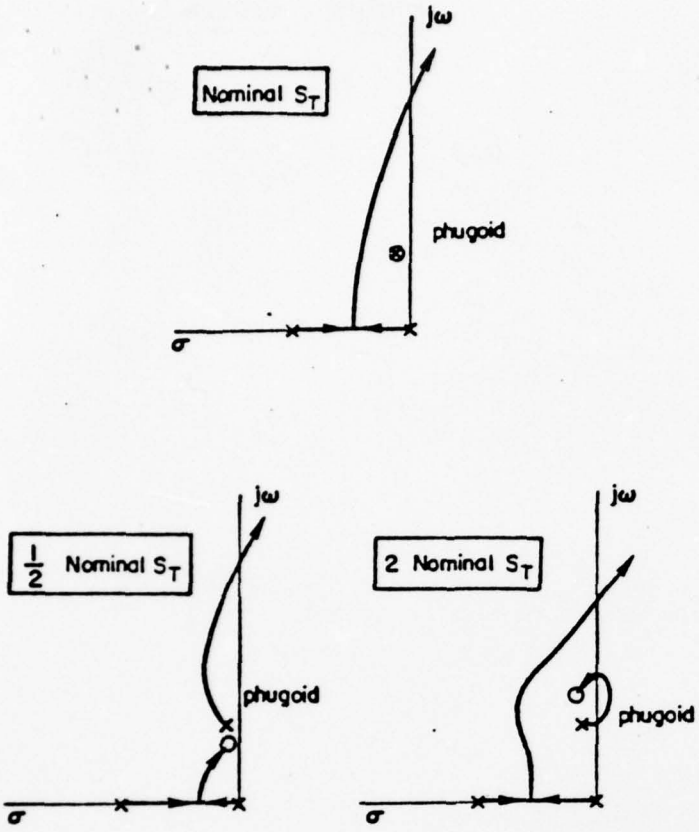

Figure 19. Decoupled Airplane Altitude Control (h/h_c) Characteristics with S_T Variation.

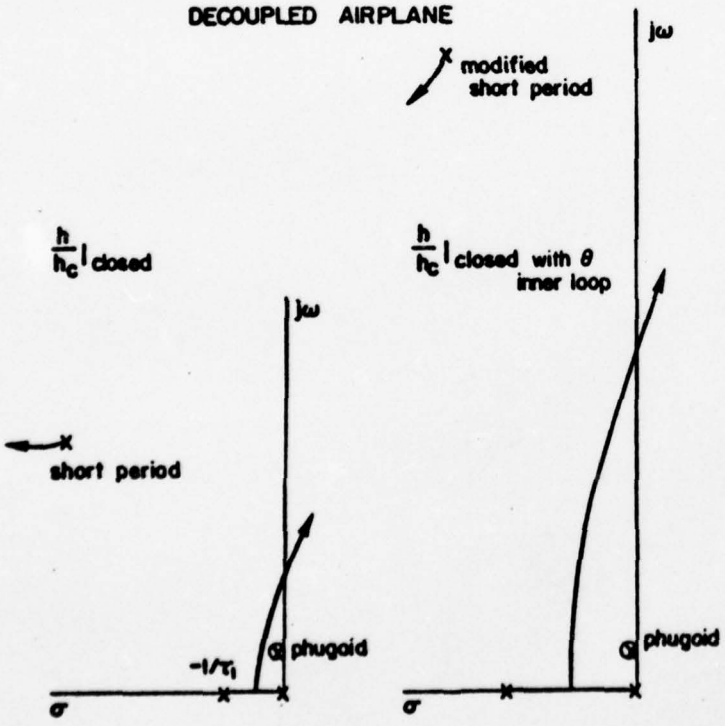

Figure 20. Decoupled Airplane Altitude Control with Pitch Attitude Inner Loop.

Therefore if the simple altitude closure with the decoupled airplane does not give sufficient bandwidth, it may be possible to improve the bandwidth by closing the inner pitch attitude loop.

Effects of Off-Design Center of Gravity Position

A c.g. shift results in an off-design condition because both the throttle to stick and stick to throttle crossfeed gains are functions of the static stability, M_α. It was shown in Section 2 that S_T is proportional to $1/M_\alpha$ and T_s is directly proportional to M_α. Thus, for an aft c.g. off-design condition ($|M_\alpha|$ smaller), for example, the amount of throttle due to stick would be too small and an unwanted transient in speed response (phugoid excitation) would occur; likewise, T_s would be too large and too much elevator would be applied for throttle inputs, causing a steady state flight path error as well as an unwanted transient response (phugoid excitation).

Open Loop Response Characteristics - Figures 21a and 21b, show time histories of the decoupled airplane's response to step inputs of the γ and V controllers at 10% mac forward and 10% mac aft c.g. positions.

The treatment of the open loop response characteristics will first consider γ controller inputs. The essential difference between the c.g. forward and aft case is the amount of transient excitation in the γ response (shown in Figures 21a and 21b). Clearly the aft case exhibits a more rapid response and has much more phugoid excitation than the forward case. Pilots might possibly prefer the forward case over the aft case since there is less transient excitation.

The above discussion may be clarified by considering Figures 22 and 23. Figure 22 is a pole-zero sketch for the γ controller. This diagram depicts the relative locations of the phugoid pole and zero varying M_α. At the design value of $M_\alpha(-6.1)$ a near perfect pole zero cancellation is achieved. Figure 23 shows the open loop $j\omega$ Bode magnitude plots for the three c.g. positions. The almost first-order like properties can be seen in the nominal case. The relative positions of the phugoid numerator and denominator change for the c.g. forward and aft cases.

It is also interesting to notice the direction of the transient speed response due to γ controller inputs. For the c.g. forward case speed initially decreases, but there is, of course, no steady state error. The

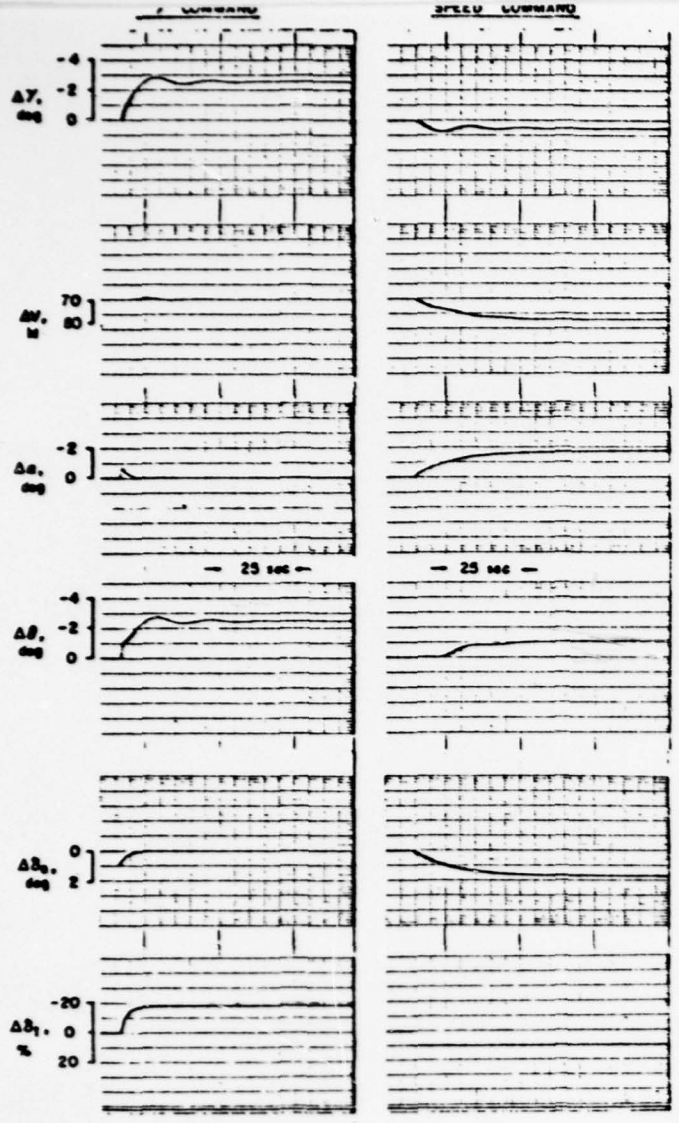

Figure 21a. Time Histories of Decoupled Airplane; 10% Forward C.G.

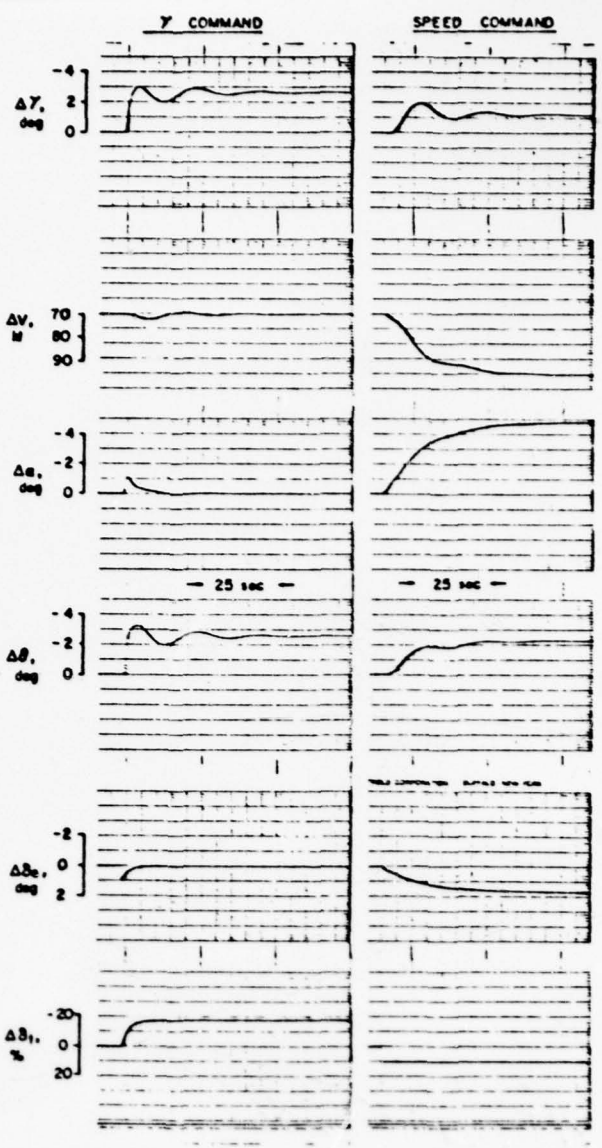

Figure 21b. Time Histories of Decoupled Airplane; 10% Aft C.G.

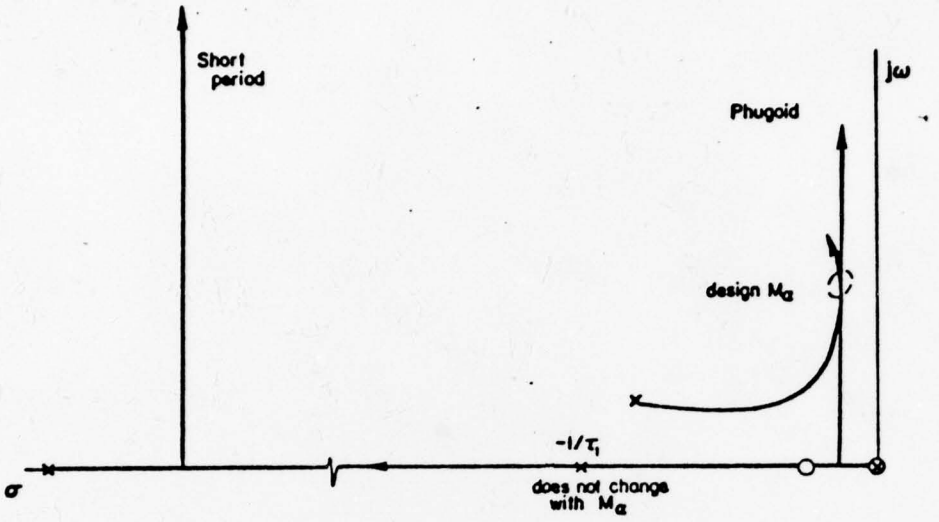

Figure 22. Locus of Poles and Zeros for γ Controller Varying M_α.

transient may be explained as follows: S_T is larger than necessary (c.g. forward) so the decoupler will reduce power (or increase as the case may be) more than necessary resulting in a slight speed decrease transient. The opposite is true in the c.g. aft case.

Now consider what happens for speed controller inputs. Center of gravity either forward or aft will result in some steady state γ errors because T_s will either be too large or small. Recall that T_s is the parameter that controls how much elevator is applied for throttle (speed controller) inputs. The magnitude of the steady state speed response will depend on M_α. A c.g. shift forward results in a smaller steady state response for speed controller inputs than for a c.g. shift aft (shown in Figures 21a and 21b).

The magnitude of the steady state response may also be observed in the open loop Bode magnitude plots for the speed controller (Figure 24). The steady state value is simply the Bode or d.c. gain and it is seen that the Bode gain is larger (+) for the c.g. aft case.

The pole-zero sketch for the design speed controller (again varying M_α) shows the pole-zero cancellation in the phugoid region (Figure 25). However,

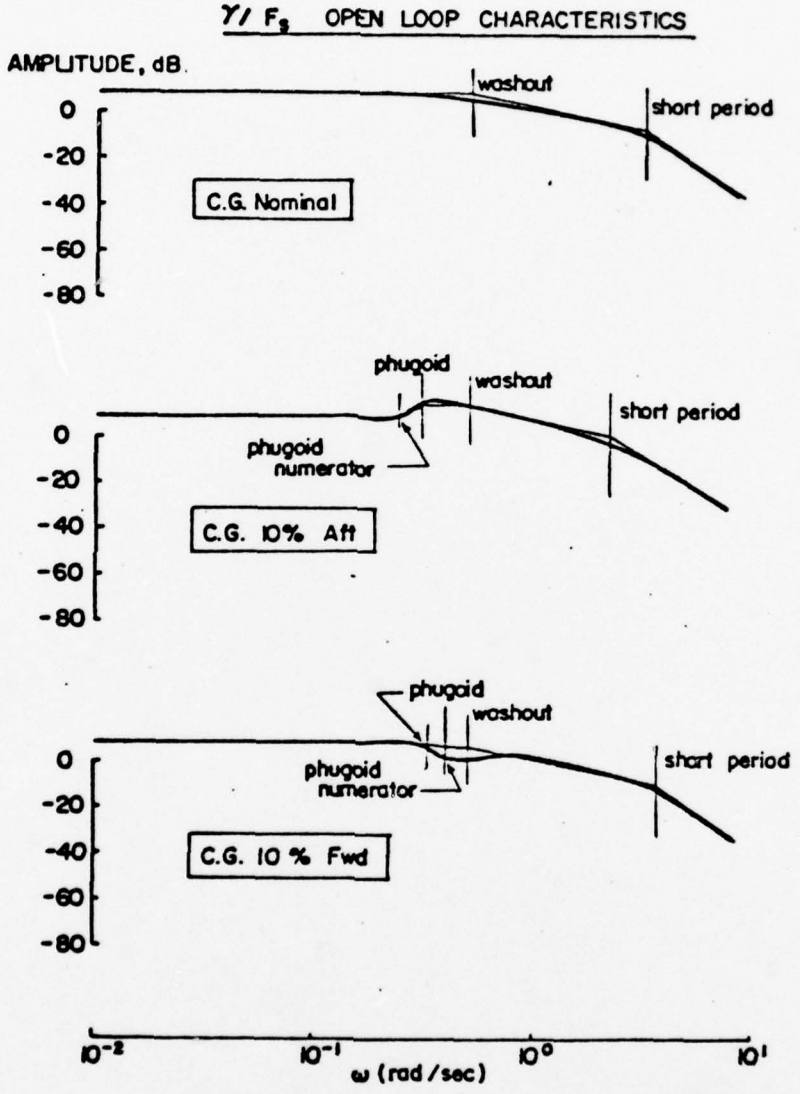

Figure 23. γ/F_s Open Loop Bode Charateristics; C.G. Variation.

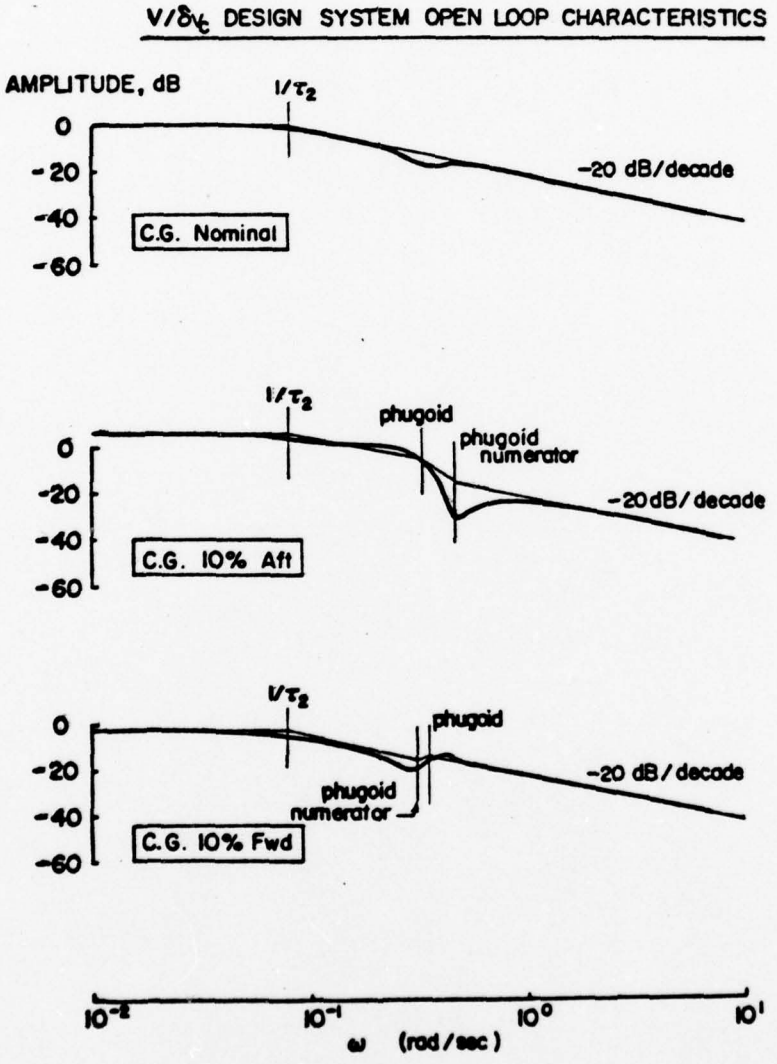

Figure 24. V/δ_{vc} Open Loop Bode Characteristics; C.G. Variation.

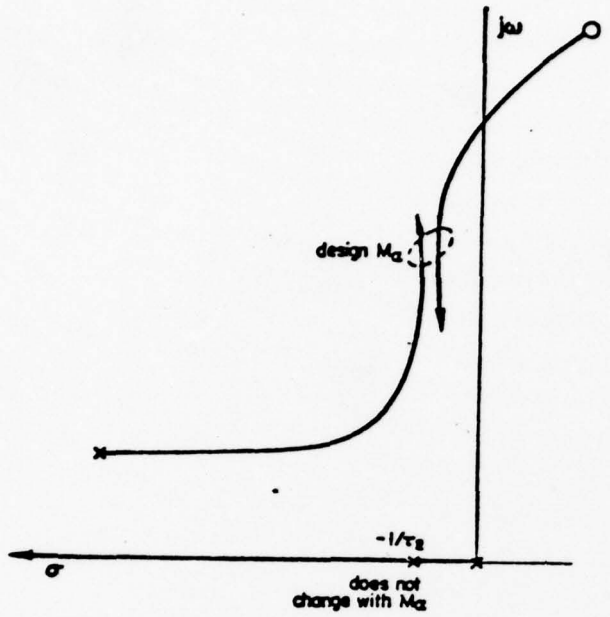

Figure 25. Locus of Poles and Zeros for Speed Controller Varying M_α.

at $M_\alpha = 0$ it is noticed that there is a non-minimum phase zero which will surely result in control problems for the pilot. The indicated cross-over occurs at a level of M_α between -2.0 and -3.0. This indicates that the speed controller is more sensitive than the γ controller to aft c.g. positions.

The sign of the steady state γ error will also probably influence pilot opinion of the speed controller. Figures 21a and 21b show that for a speed increase command the c.g. forward case results in a + γ transient and steady state response while the opposite is true for a c.g. aft case.

Piloted Airplane Altitude Control - Root locus sketches for a simple altitude loop closure by the pilot are shown in Figure 26. The criterion for closure was a phase margin of 40° and the root locations in the phugoid region are indicated on the sketches.

The closed loop Bode Plots shown in Figure 27 would seem to indicate a little more bandwidth in the aft case than in the forward case. The difference in bandwidth of all three cases still is not significant which indicates that the pilot opinion for these cases may not differ drastically.

Certainly at large aft c.g. positions short period dynamics would degrade to the point that the pilot would prefer forward cases.

At this point it may also be worth mentioning a simple flight path angle closure by the pilot. Normally γ cues are very difficult for the pilot to sense. The analysis of a simple γ closure (assuming that γ information is available to the pilot) indicates that more bandwidth is available

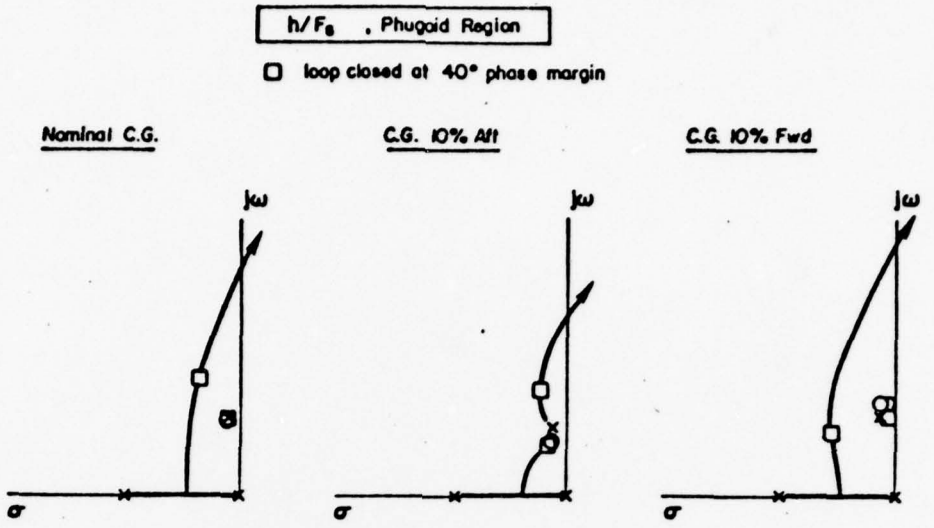

Figure 26. Decoupled Airplane Altitude Control Characteristics With C.G. Variation.

for the c.g. forward case. This is due mainly to the improvement in short period dynamics (ω_{sp}). It may be possible for the pilot to obtain good γ information via the pitch attitude variable. In the steady state and at low frequencies (phugoid) γ is essentially equal to θ for the simplified decoupled controller.

Decoupled Airplane With the One-Motor System

When the pilot concentrates on glideslope tracking, and this is generally true for the approach, it is possible that the pilot would not notice the difference between the one-motor system and design system. The essential difference between the one-motor and design system is that there is γ coupling but since the pilot is active in the γ loop he will suppress any γ deviations.

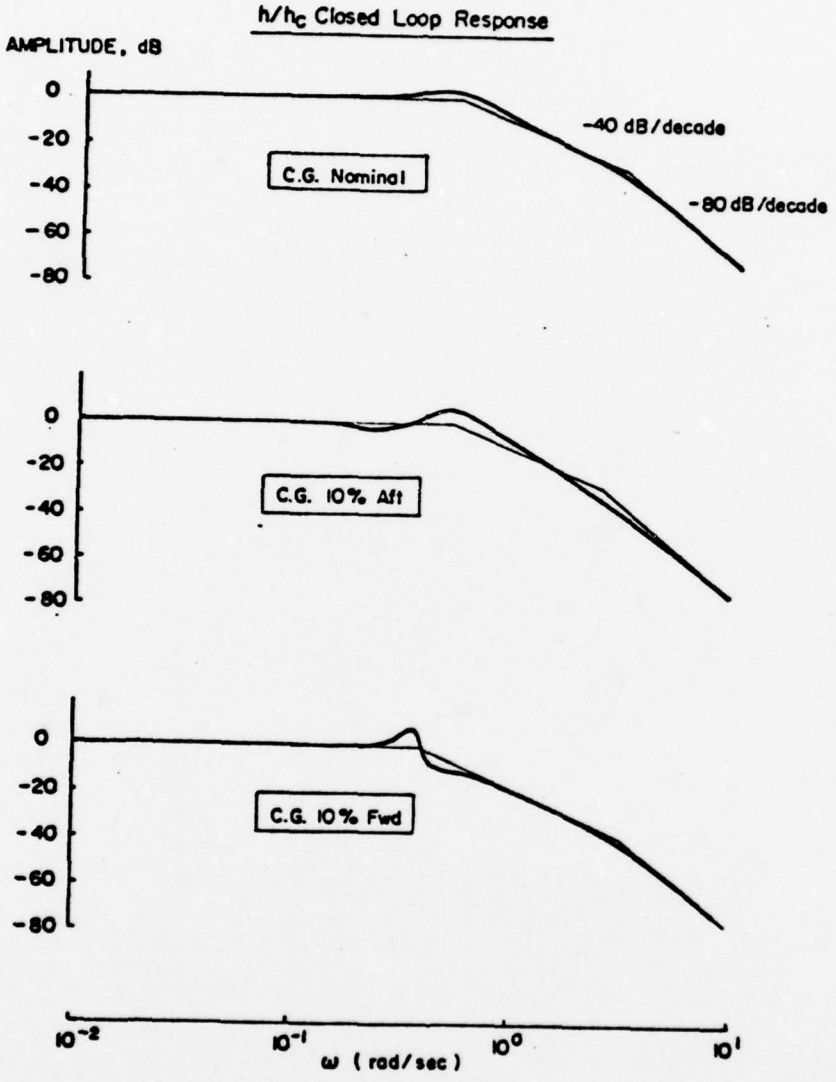

Figure 27. Closed Loop Altitude Control Bode Magnitude Diagram for Piloted Decoupled Airplane With C.G. Variation.

SECTION 4

PRELIMINARY INVESTIGATION

General Description

Prior to the in-flight simulation, a preliminary evaluation of the decoupled system was accomplished by use of a ground-based simulator. The numerical values of the stability derivatives of the Navion (Appendix C) were used. The purpose of these experiments was to explore the general utility of the system. The effects of c.g. shift and τ_1 variation were investigated to get some idea of what would follow in flight. A few runs in simulated turbulence were also tried again to try and gain a preliminary qualitative feel for its effect.

Description of the Experiment

The block diagram representation of the ground-based simulator is shown in Figure 28. A hydraulic force-feel stick and a throttle handle with position sensing served as pilot controllers.

Test Configurations - Three different values of stick washout time constant τ_1 were selected for investigation based on the results of previous work (Reference 9). The values used were 1, 2 and 3 sec.

Center of gravity position was varied about the nominal (25% mac) position. Shifts of ±10% mac as well as some runs with the c.g. at the neutral point ($M_\alpha = 0$) were investigated. Center of gravity position is an important design condition since the crossfeed gains depend on the level of static stability (M_α).

The sensitivity of the altitude indicator (glideslope deviation) was varied to simulate sensitivity of a glideslope indicator to ILS range. It was initially thought that pilot opinion of the decoupled system would be strongly influenced by the parameter, but the fixed base results indicated that this was not the case.

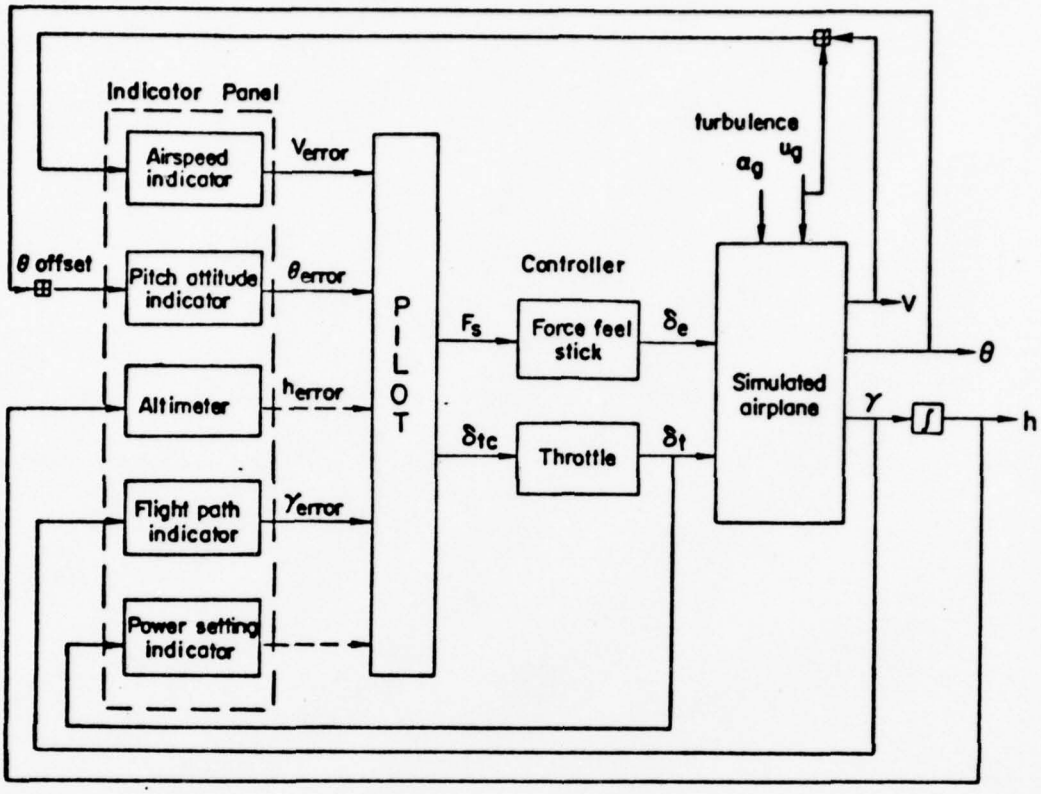

Figure 28. Block Diagram Representation of the Ground Based Simulator.

The only other parameter that was varied was the level of simulated turbulence. Moderate and heavy turbulence were selected as the levels for simulation.

Flight Task - Where turbulence was not used, pilots were asked to create their own offset or error and to evaluate the system according to the Cooper-Harper scale (Appendix B). Pilots evaluated the various configurations according to the ease with which they could return to the nominal condition. The basic airplane (Navion with conventional stick and throttle) served as a baseline configuration.

Results - The results of the experiment where τ_1 was varied are shown in Figure 29. Pilots indicated a preference for the 2 second value. The results of the c.g. shift experiment are shown in Figure 30. The degradation

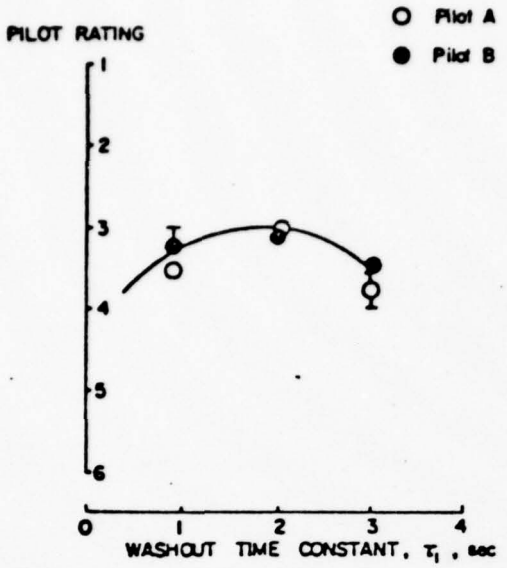

Figure 29. Effect of Washout Time Constant on Pilot Rating; Ground Based Simulation.

in pilot opinion for both the decoupled and basic configurations at aft c.g. positions is indicated. Conclusions about flight in turbulence were difficult, since the pilots seemed to rate the decoupled and basic airplane about the same.

Several simulations were conducted to explore the difference between one-motor system and design system; no significant differences were observed between two systems as predicted in Section 3 for either nominal c.g. position or ±10% mac c.g. shift.

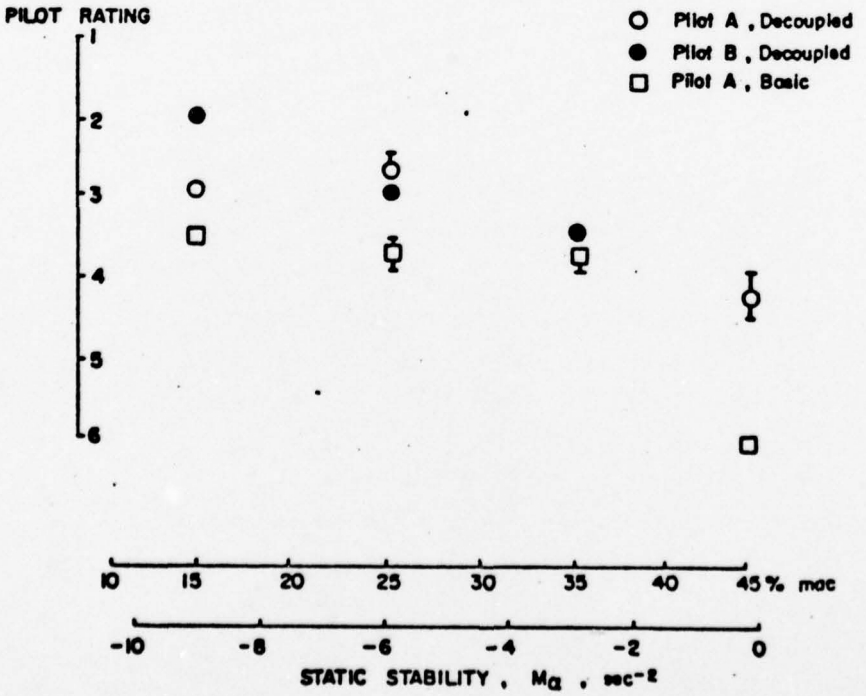

Figure 30. Effect of C.G. Shift on Pilot Rating; Ground Based Simulation.

SECTION 5

IN-FLIGHT SIMULATION

In-Flight Simulator

The test vehicle used in the study is a highly modified Navion (Figure 31). In its present form it is a "fly-by-wire" airplane with variable stability and control characteristics in all degrees of freedom except that

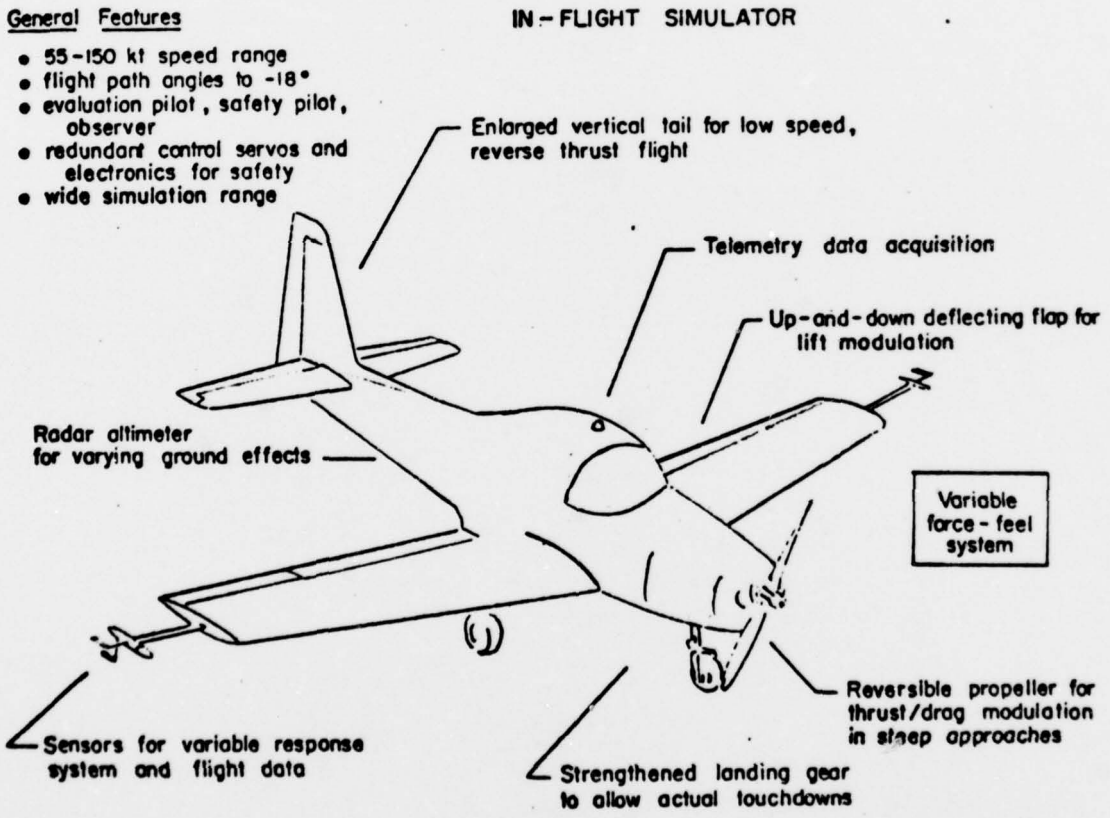

Figure 31. Variable Response Navion In-Flight Simulator.

of sideways motion. Flight in turbulence can be simulated by supplying forcing signals representing vertical, side and fore-and-aft gust components to the control surfaces. The rms gust magnitude can be varied from zero to 1.8 m/sec (6 ft/sec).

The cockpit interior of the airplane is shown in Figure 32. The left seat is occupied by the evaluation pilot and is equipped with a standard set

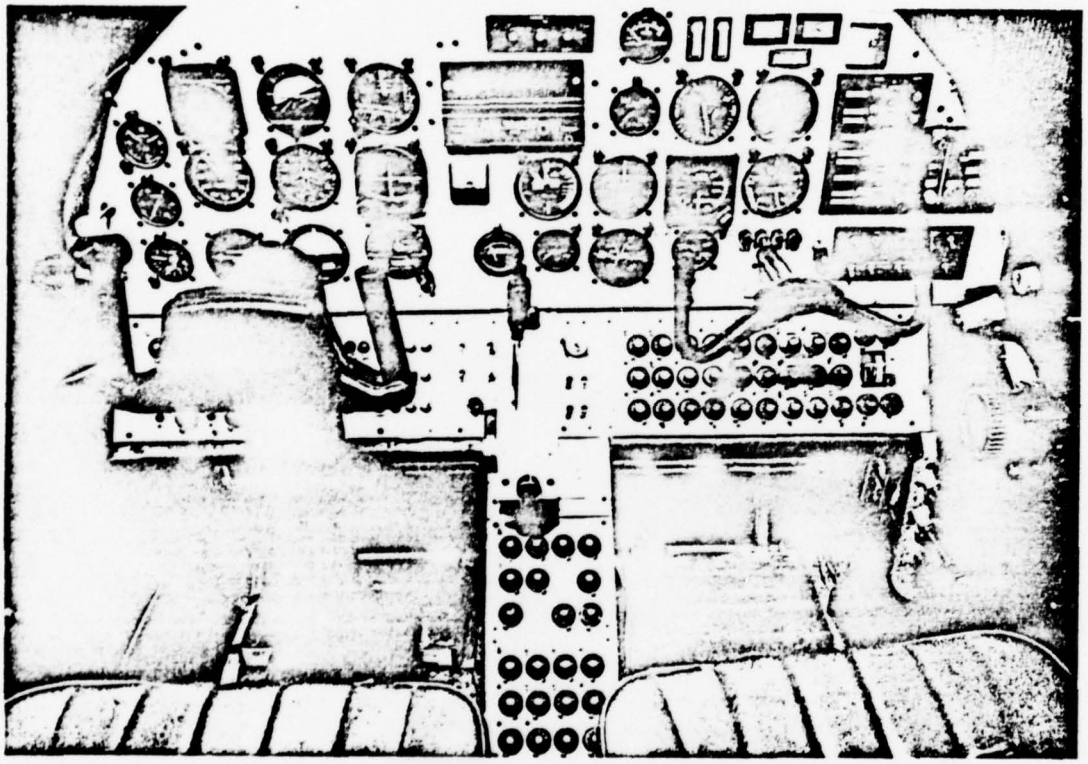

Figure 32. Cockpit Interior of In-Flight Simulator.

of blind flying instruments. The left seat is also equipped with a force-feel controller (Appendix A). This system gives the capability of simulating control system characteristics such as the control force gradient, natural frequency, damping ratio, breakout forces, downspring and bobweight characteristics. The quadrant-style throttle is also shown.

A means of trimming the stick was provided via a beep trim system. With the decoupled system engaged, the pilot would be required to hold a constant

force after making a flight path angle change (if no means of trim was available). The beep trimmer essentially nulled the electronic force signal of the force-feel stick.

The right seat is occupied by a safety pilot who sets up the various conditions including the selection of the decoupled or basic system. The safety pilot's controllers are the standard Navion mechanical stick and throttle.

Flight Task and Evaluation Variables

Both VFR and IFR approaches were set as evaluation tasks. The basic airplane was considered as a baseline with which the decoupled airplane variations were compared.

The pattern flown was a conventional airplane traffic pattern with downwind, base and final legs. Normal procedure was to engage the decoupled system after the final turn but prior to interception of the glideslope (for IFR tasks). A typical IFR pattern depicting the normal sequence of events is shown in Figure 33. VFR patterns were essentially the same except there was, of course, no localizer or glideslope interception.

The pattern shown in Figure 33 is typical of most runs flown although several variations were often introduced. As experience with the system grew, the evaluation pilot often took the controls on the downwind leg and flew the system around the downwind-base and base-final turns. Pilots accomplished the turns with little or no difficulty, commenting that with the system engaged they tended to fly a little fast around the turn. System engage was usually accomplished at the 70 kt speed, but higher speeds were often used as initial conditions.

The primary data considered of evaluation pilot ratings (Reference 12 and Appendix B) and commentary. Measurements of airplane motions, tracking performance and pilot inputs (stick force and throttle motion) were relayed to ground by means of telemetry. The bulk of the evaluations were done by two Princeton test pilots; several other pilots both with and without testing background also flew the decoupled airplane.

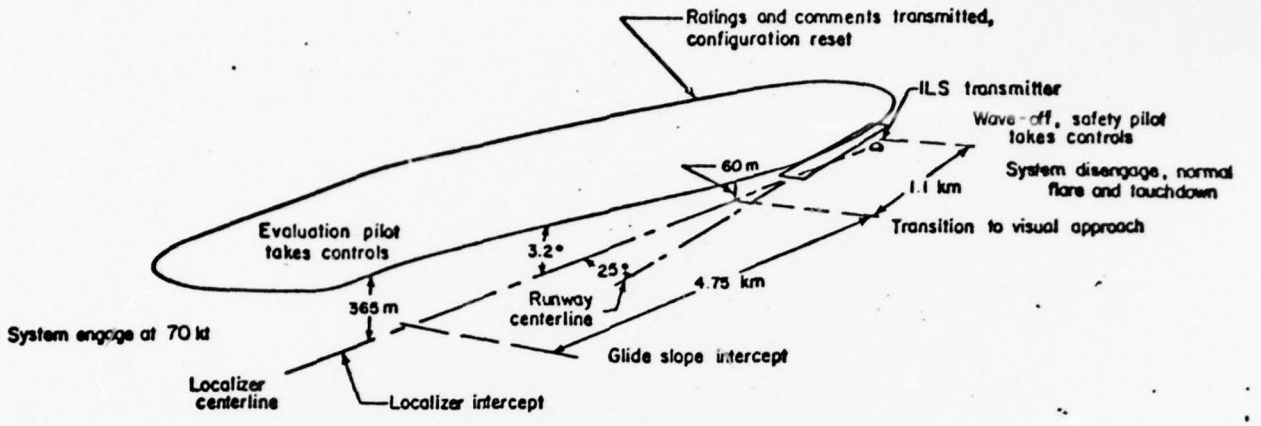

Figure 33. Flight Pattern.

Test Variables

The flight test program contained the following parameter variations:

Stick Washout Time Constant (τ_1) - Three stick washout time constants for the decoupled system were selected for evaluation on the basis of earlier ground based simulation tests. The values were 1 sec, 2 sec (moderate, expected to be best), and then 3 sec (slow).

Off-Design Center of Gravity - The c.g. position is known to have a major affect on longitudinal flying qualities in general, and for the decoupling system it becomes a design condition. Several c.g. positions were selected between 10% mean aerodynamic chord (mac) forward and 20% mac aft of the nominal case as shown in Figure 34. The Navion loading diagram is shown in Figure 35.

Flight in Turbulence - Light (σ_g = .9 m/sec) and moderate (σ_g = 1.8 m/sec) turbulence levels were simulated during some runs. Tests were also conducted in (unmeasured) natural conditions ranging from calm air to qualitatively heavy turbulence.

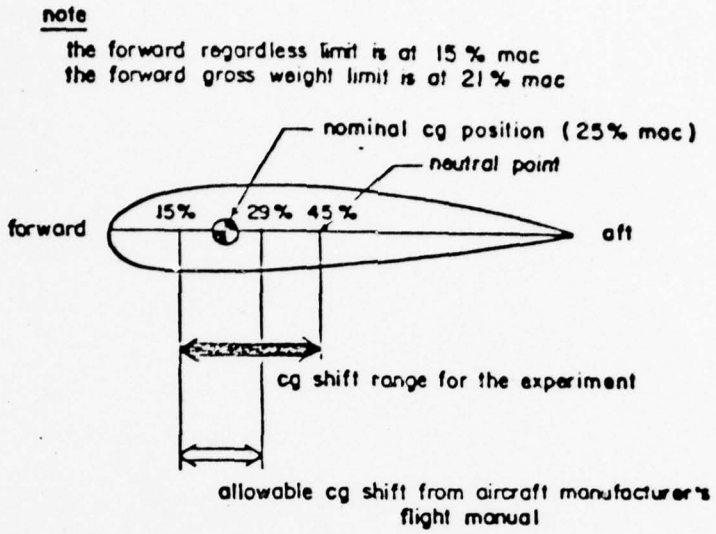

Figure 34. C.G. Shift Range for the Experiment.

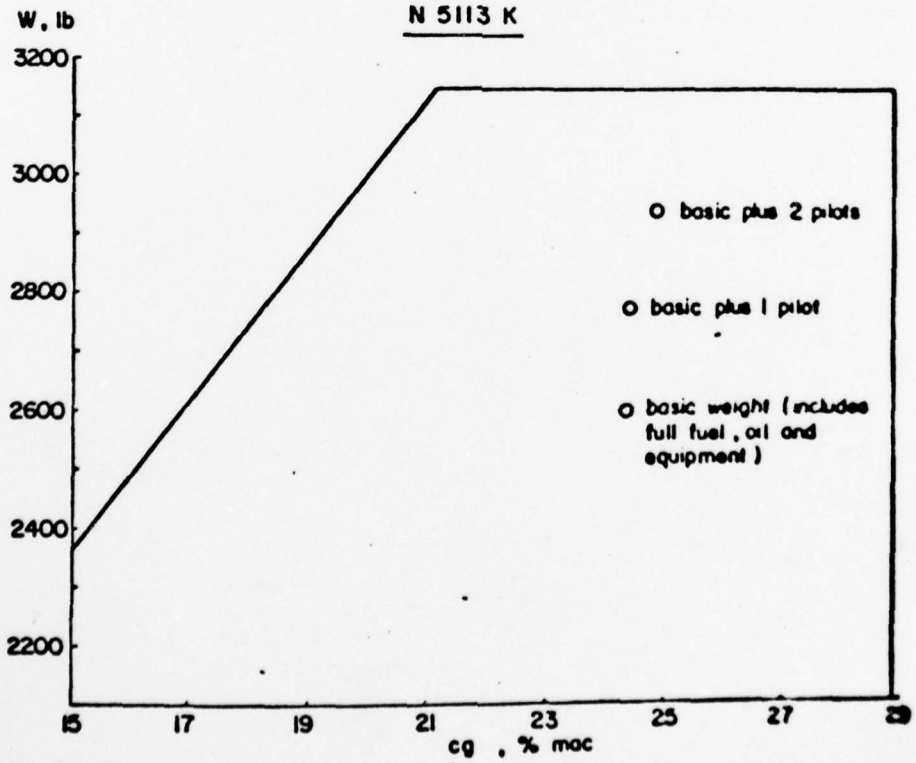

Figure 35. Navion Loading Weight — C.G. Envelope.

Off-Design S_T and τ_2 - Both S_T and τ_2 are known (see Section 2) to have an affect on the phugoid excitation for γ and speed command inputs respectively. Of particular interest is an off-design S_T value for flight in turbulence. This particular effect was explained in Section 3.

Flight With One-Motor System - Several runs with the one-motor system were conducted to be compared with the designed decoupled system.

SECTION 6

RESULTS AND DISCUSSION

Flare and Touchdown With Decoupled Airplane

Preliminary trials indicated that although the approach handling characteristics of the decoupled airplane were promising, there would be some fundamental difficulties with the flare and touchdown. The nose-down pitching moment due to ground effect caused more elevator — and hence more power — to be used in the flare than would have been used to make the same flight path angle change on the approach. The result was a tendency for the airplane to accelerate and assume a nose-down attitude during the landing. Attempts to counter this with a speed reduction command were generally unsuccessful due to the long (12 sec) ime constant of the speed response mode. In view of these difficulties,it became normal procedure to disengage the decoupled system at or slightly above the flare point and land normally. It might be pointed out that a production version would most likely provide a mechanical throttle override capability with which the pilot could prevent unwanted power increases in the flare. At any rate, the pilots felt that there was nothing intrinsically wrong with the pre-landing disconnect which is similar to autopilot practice.

Selection of Optimum Stick Washout Time Constant

The results of an experiment to determine the optimum stick washout time constant are presented in Figure 36. A preference for a value of approximately

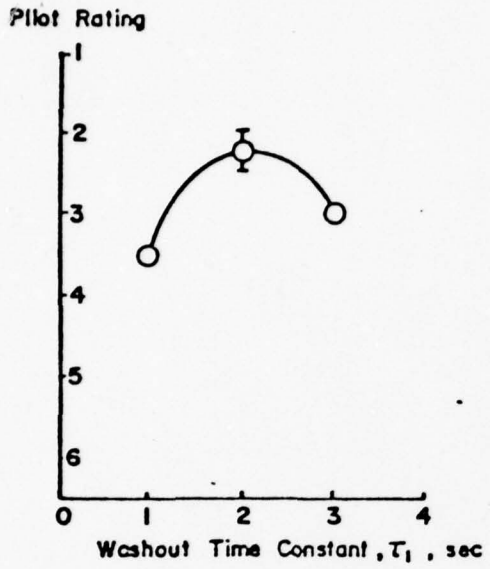

Figure 36. Effect of Washout Time Constant on Pilot Rating; In-Flight Simulation.

2 seconds is indicated. Although the pilot/airplane system analysis of Section 3 suggested that $\tau_1 = 1$ sec might be best from a performance standpoint, it was found in flight that the control motion was so obvious and rapid as to be annoying. The pilot noted that he had to concentrate on not resisting the washout in order to make smooth glidepath corrections; this factor was not present with the two longer time constants. In all cases glideslope tracking performance was judged to be satisfactory. The value $\tau_1 = 2$ sec was selected for the remainder of the program.

Comparative Evaluations in Nominal Conditions

(Smooth air and c.g. at 25% mac)

Flight test results show a clear preference for the decoupled airplane over the basic airplane for both instrument and visual approaches as predicted by the pilot/airplane system analysis in Section 3. Table 2 presents the basic airplane versus decoupled airplane ratings in nominal conditions. The three evaluation pilots flew the system on different days.

Table 2. Pilot Ratings for Decoupled and Basic Airplane

PILOT	TASK	DCPLD AIRPLANE	BASIC AIRPLANE
A	VFR	1½ - 2	3½ - 4
B	IFR	2½ - 3	3 - 3½
C	VFR	1½ - 2	2½
C	IFR	2	2½

Pilots commented favorably on the easy precise glideslope tracking with lowered workload. Specific factors were the following:

- Benefit from quick response, predictable steady state
- Glideslope tracking done with single control using simple fly-up-or-down logic; comparable performance with conventional controls would have required careful continuous coordination of both stick and throttle.
- Small airspeed excursions; speed can assume a low priority in the instrument scan.
- Glideslope deviation or rate of descent cues can be used directly; although pitch attitude will change, it need not be included in the instrument scan as a means of controlling either descent rate or speed.

Normally, the desired speed would be set at the beginning of the final approach leg. One important question which must be considered involves the allowable level of airspeed excursion about the nominal value. The pilots who flew the decoupled system all agreed that airspeed excursions of 1 to 2 kt were of little significance, and up to 5 kt might be acceptable if on the fast side. It should be pointed out that the better rating for the decoupled airplane does not necessarily indicate a better performance; a good pilot can achieve the precise coordination necessary for glideslope tracking and holding airspeed within 1 to 2 kt with the basic airplane, but at the expense of higher workload. Figure 37 shows time histories of both the decoupled and basic airplanes for VFR approaches. The essential difference between the two runs is that throttle manipulation is evident with the basic airplane while in the case of the decoupled airplane it is not.

Although the above results are specifically for straight-in, constant-speed approaches, a few trials indicated that medium-banked (20^{o}) turns and moderate decelerations during the approach could be accomplished without difficulty. Initial speeds of up to 100 kt were used, with the reduction to 70 kt usually beginning at about 61 m (200 ft) altitude.

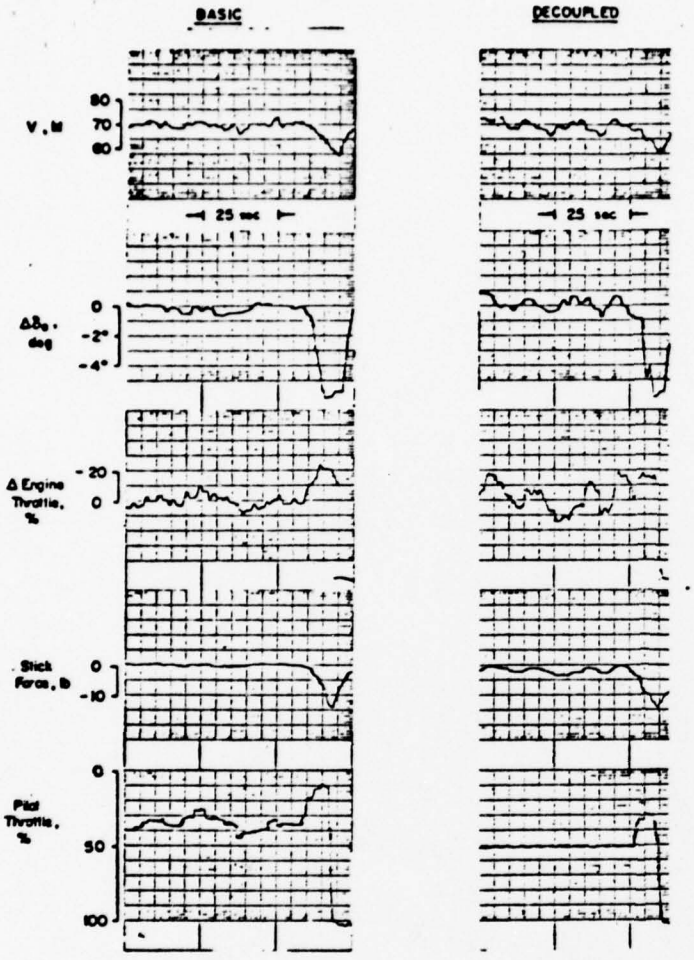

Figure 37. Flight Test Time Histories of the Decoupled and Basic Airplanes.

Effects of Flight in Turbulence

The pilot rating results of flight in simulated turbulence are shown in Figure 38. For low levels of turbulence, the decoupled airplane was rated better than the basic airplane. As the turbulence level increased, the pilots began to indicate a preference for the basic airplane due mainly to problems in controlling the long period (phugoid) velocity changes which were excited by gust inputs (by design, control inputs by themselves do not excite the phugoid mode, as discussed in Section 3).

Figure 38 is meant to show the trend of pilot rating in turbulence; the crossover point should not be interpreted as always occurring at the 1.5 m/sec rms level of turbulence. The curve does indicate that in heavier turbulence pilots begin to indicate a preference for the basic airplane.

The difference between the decoupled and basic airplane is only one-half rating point, and although this might not seem very significant, it should be noted that the results were obtained in somewhat idealized conditions with few distractions. For instance, at the VFR transition point the pilot always presented with an obstruction-free runway, and there were no restrictions to visibility caused by weather or night conditions. No other airplanes were in the pattern and the pilot

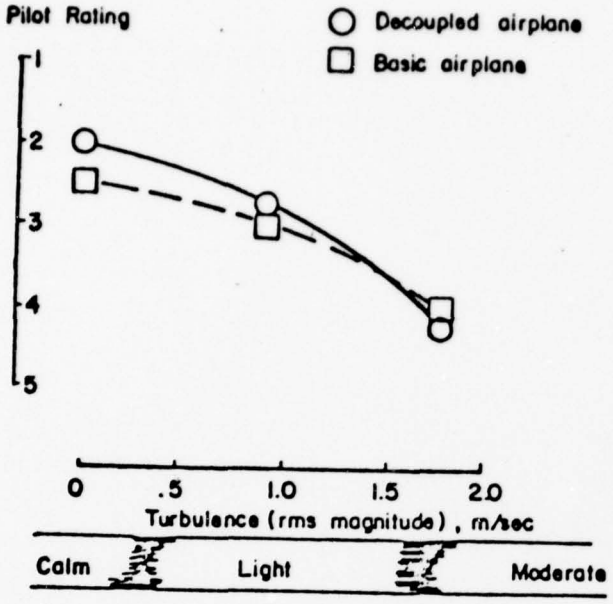

Figure 38. Effects of Flight in Turbulence on Pilot Rating IFR Task.

was not required to handle communications with a control tower or be prepared for an IFR missed approach procedure. It seems likely that if the results were extrapolated to a "real world situation" the difference in rating would be greater.

In low levels of turbulence, the pilots tended to ignore small airspeed and pitch attitude excursions and concentrated on holding the desired glidepath. In heavier turbulence, however, big upsets occasionally led to large amplitude, long period oscillations in speed, attitude and flight path (phugoid motions) which were impossible to ignore. In most cases the pilots could suppress the flight path excursions by giving full attention to path control, though they found it impossible to suppress the speed excursions by using the stick (as explained in Section 3). Figure 39 shows the time histories of an approach in turbulence in which the pilot performed the glideslope tracking task adequately by using the stick, although about ±3 kt speed excursions can be observed. In cases where larger speed excursions occurred, the pilot expressed a desire to revert to conventional pitch control to suppress the large attitude excursions and thus damp the phugoid. This technique is also discussed in Section 3.

Based on the pilot/airplane analysis, several flights were conducted to evaluate the effects of S_T on suppressing the phugoid mode excited by turbulence. There was a slight improvement in pilot rating by setting S_T at half of the nominal value. In moderate levels of turbulence (1.8 m/sec rms), a rating of 4.0 was given to both the basic and decoupled airplanes.

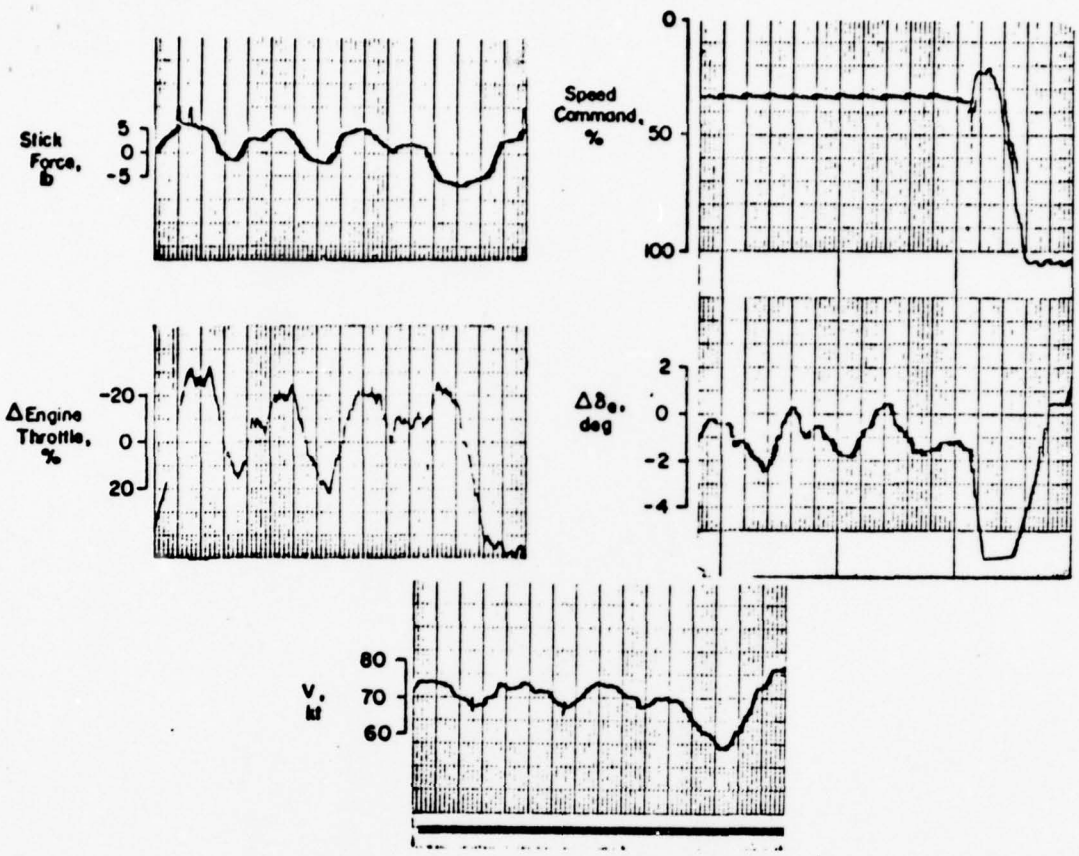

Figure 39. Decoupled Airplane Time Histories of Flight in Turbulence.

In principle it should be possible to help damp speed excursions in the decoupled case by using the speed controller, but the pilots found this to be nearly impossible in situations where the airplane was being constantly upset. They commented on the difficulties of controlling two variables (speed in addition to glideslope) simultaneously, and also identified deficiencies in the speed controller such as the lack of calibration (kt per unit of deflection) and inability to identify the trim point by feel.

The long time constant also contributed to the problem by making it difficult to see or predict the effects of the control inputs. An attempt to improve the speed response was made by setting $\tau_2 = 5$ sec, while still retaining steady state decoupling. A recent study (Reference 3) showed that shorter time constants in speed response (5 sec in a completely decoupled STOL configuration) gave better pilot ratings. The root locus

analysis of the simplified decoupled airplane (Figure 40), however, shows that the modified phugoid mode might become more lightly damped. Flight test results with τ_2 = 5 sec produced poorer ratings for flight in turbulence. The pilots suggested the possibility of overdriving the speed controller to get a faster speed change, but several attempts were unsuccessful due mainly to the unpredictability of the speed response.

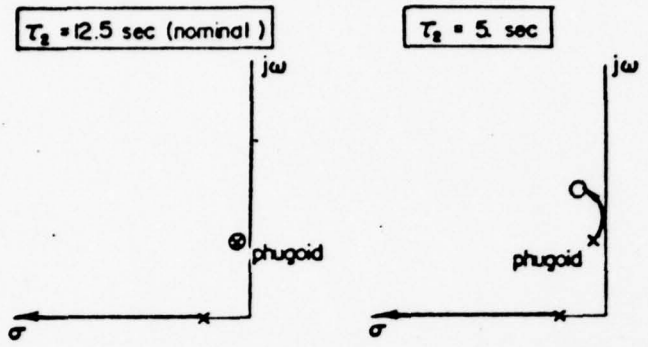

Figure 40. V/δ_{V_C} Root Locus Sketches; τ_2 Variation.

Compared to the Reference 3 results, the degradation of pilot rating for the simplified decoupled airplane in light turbulence is about the same as for the completely decoupled STOL configuration which was considered to have a low sensitivity to such disturbances.

Effects of Off-Design Center of Gravity

The pilot rating results for tests with off-design c.g. position are presented in Figure 41. Forward c.g. shifts offered no particular problem to the pilots and they could perceive little difference between the nominal and forward cases. This is supported by the pilot/system analysis in Section 3 where it was shown that the closed loop bandwidths in these two cases were about the same.

Aft c.g. movements ($|M_\alpha|$ smaller) proved to be more bothersome; for small shifts (within manufacturer's prescribed weight and balance), the decoupled airplane remained better than the basic airplane. At far aft off-design conditions the basic airplane received a better rating, but this occurred with a level of M_α which was well outside of the allowable envelope.

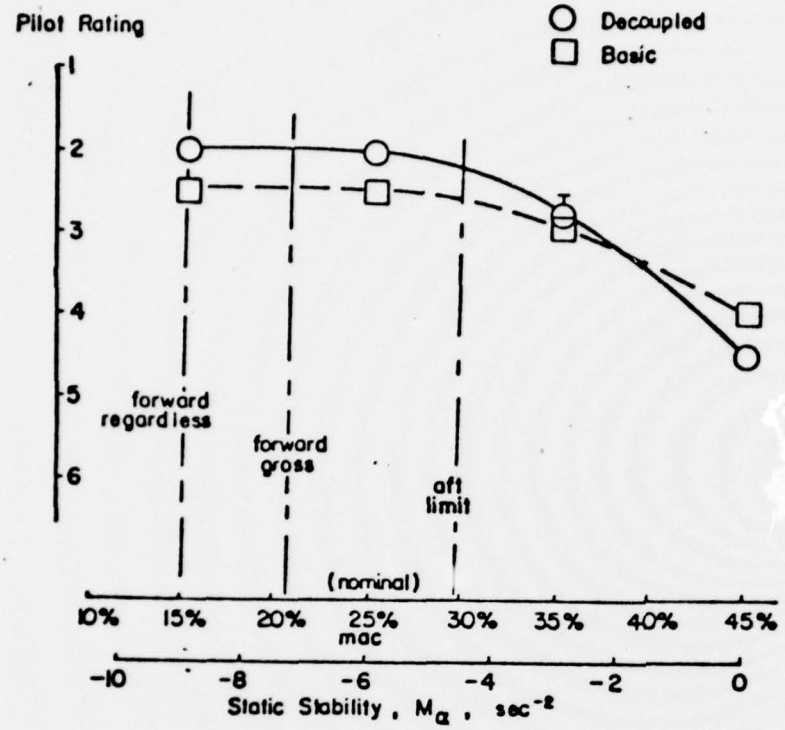

Figure 41. Effects of C.G. Shift on Pilot Rating.

In terms of performance, the evaluation pilot was still able to adequately perform the task of glideslope tracking using stick only with $M_\alpha = 0$. However, use of the speed controller with $M_\alpha = 0$ excited such large transient pitching motions that pilots preferred not to use it. The pilot/system analysis in Section 3 showed that much more elevator (due to throttle) is supplied than necessary, which is the same as saying the crossfeed gain T_s is too large. At extreme aft c.g. positions ($M_\alpha = 0$), the presence of the nonminimum phase zero in the $\Delta V/\Delta\delta_{Vc}$ transfer function accounts for the difficulties encountered in flight.

Combined Effects of Turbulence and Center of Gravity Position

The pilot rating results for runs with off-design c.g. in turbulence are presented in Figure 42. For this experiment, M_α was set at -3.0 (c.g. located at 35% mac). The results show that the workload involved in flying the basic and decoupled airplanes is nearly the same. Airspeed excursions, though within tolerable limits, were probably large enough to have some effect on glideslope tracking and required some attention. The overall effect was to make the workload comparable to the basic airplane.

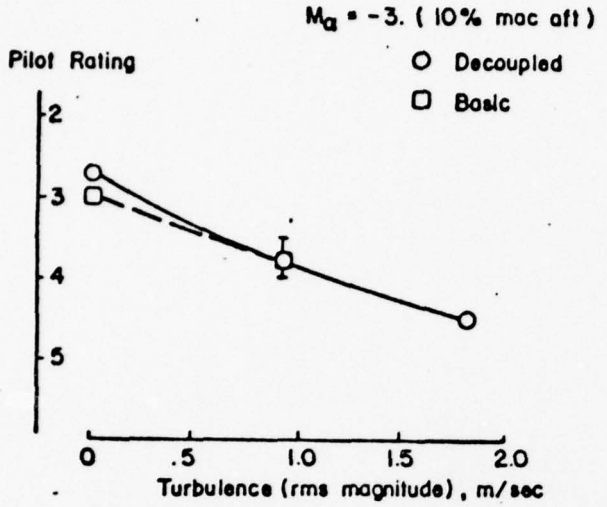

Figure 42. Combined Effects of Turbulence and C.G. Position on Pilot Rating.

Decoupled Airplane With One-Motor System

A few flight test results showed that the pilot did not notice any significant difference between the one-motor system and the design system as expected from the pilot/airplane analysis. A brief look at the one-motor system during the preliminary investigation indicated that the γ coupling was not significant when the pilot was actively controlling flight path.

Effects of Natural Airplane Coupling Parameters

To simplify the experiment, the in-flight simulator was adjusted so that pitching moments due to thrust variation ($M_{\delta t}$) and speed variation (M_V) were zero. If present, a pitching moment due to thrust would cause the decoupled system to have a steady state speed error for a γ command or a flight path error for a V command. To correct this situation in an actual system, the washouts could be made to overshoot enough to exactly cancel the moment due to thrust (Figure 43).

The effect of significant pitching moment due to speed change could be more serious. Large positive values of M_V tend to make the phugoid mode lightly damped or even unstable, a situation not uncommon in airplanes with large downsprings in the control system. The presence of an instability would effectively prevent use of a decoupled system such as the one described here. As discussed in the section on flight in turbulence, the phugoid mode can be suppressed with respect to excitation by control action, but external forcing functions, such as gusts, will still cause

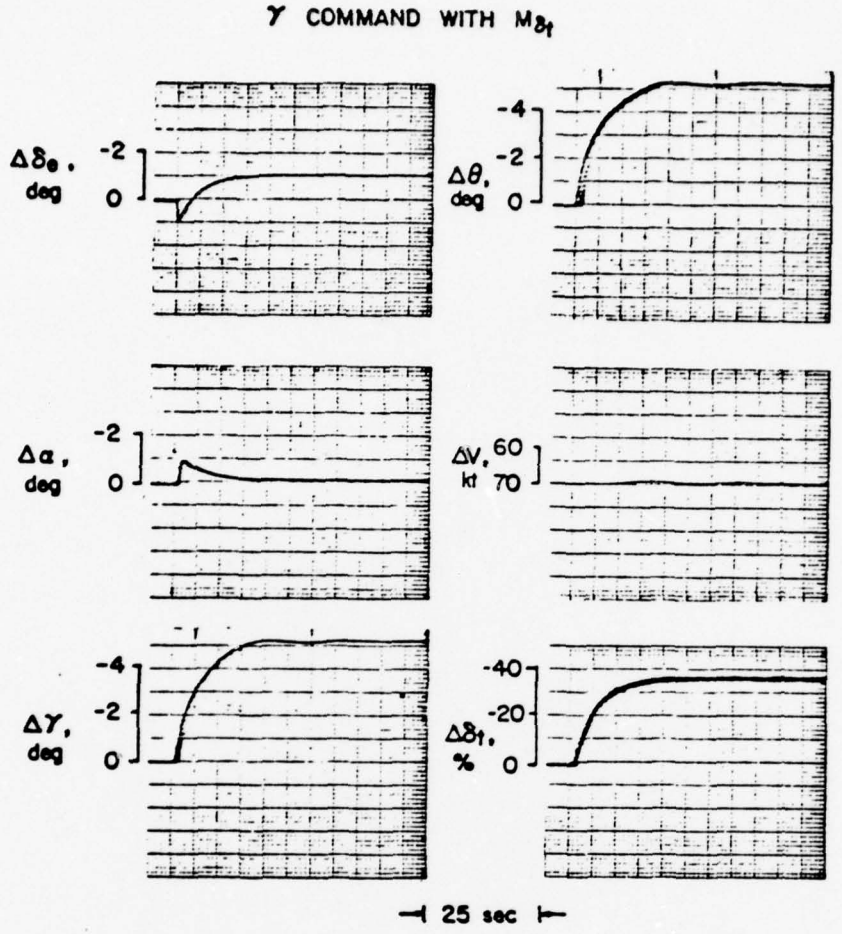

Figure 43. Time Histories of Decoupled Airplane Response with M_{δ_t} Compensation.

the motion to start.

Pitching moments due to the raising and lowering of flaps or landing gear present much less of a problem. These are simply trim changes and can be countered by appropriate use of the speed or γ controller. Alternatively, the decoupling system could be temporarily disengaged while the airplane is manually retrimmed.

Implications and Recommendations

Stick Force - An old idea was re-invented in this study — that of control force as the pilot output. The pilot was no longer required to manipulate stick position — instead he was asked to apply force to the stick. The matter of the stick actually moving while the pilot applies force is central to this decoupling scheme. The study shows that there is an optimum value for τ_1 (about 2 sec) but perhaps the most interesting point is that pilots were often not aware of the stick actually moving as they applied control force. This may indicate at least conceptually that the idea of using stick force as pilot output is a valid one.

γ Controller - The most important implication or conclusion about the γ controller is that the tolerances for good performance are quite wide. It was initially thought that it would prove to be very sensitive to c.g. position. This did not prove to be the case since rather wide variations in c.g. position (say within normal allowable limits) did not seriously effect performance or pilot opinion. The gain, S_T, was also thought to be very sensitive. Again this did not prove true. Rather wide variations (on the low side) in S_T proved to be very successful and perhaps even useful when in turbulence.

Speed Controller - Pilots were successful in using the speed controller as a discrete input device. Use of the speed controller in a continuous sense was difficult in flight. This may be in part due to the long time constant but one evaluation pilot also identified other points concerning the speed controller. (Previously listed in Results Section.)

At any rate, if the throttle is used only for biasing purposes and not in an active sense the tolerances appear to be quite wide. The one-motor system in flight was not much different from the design system despite the γ coupling. Clearly, however, more work is necessary in the domain of using the throttle in a continuous sense. A faster time response in speed without unwanted excursions would be one recommended improvement. Of course, this would require a more complicated link between the cockpit and the engine.

SECTION 7

CONCLUSIONS

A relatively simple method for decoupling the speed and flight path responses of an airplane was investigated by means of analysis and in-flight simulation. The experiments led to the following conclusions:

1) Compared with the basic airplane, the decoupled system significantly reduces pilot workload for both instrument and visual approaches under nominal operating conditions (moderate or lighter turbulence; center of gravity within normal limits).

2) Important factors in the reduction of workload are the following:

- Control functions are simplified (stick for glidepath control at constant speed; throttle for speed changes of constant flight path angle) and the need for manual coordination is eliminated.
- Glideslope deviation and rate of descent cues can be used directly; there is no need to use pitch attitude as the intermediate control variable.
- Once set at the desired value, airspeed can assume a low priority in the instrument scan.

3) Pilot workload is increased in heavy turbulence to the point where conventional rather than decoupled characteristics are preferred. Although in theory it should be possible to suppress both h and V excursions due to gust excitation by simultaneous manipulation of both decoupled controls, in practice pilots preferred to manipulate conventional stick and throttle. This is partially due to the marginal bandwidth in the $\gamma(h)$ loop as well as the pilots reluctance to devote sufficient attention to actively control speed in a closed loop sense. Use of conventional stick and throttle allowed the pilot to first close an inner pitch attitude loop helping him to suppress the phugoid.

4) Off-design c.g. positions which fall within typical normal limits will not seriously compromise operation of the decoupled system.

5) At aft c.g. positions well outside the normal limits (in particular, with M_α near zero) the decoupling is compromised and the basic airplane is preferred. Aft c.g. degrades speed control more significantly than the flight path control function.

6) During the flare and touchdown, the pilots preferred to disengage the decoupler and make normal landings. The combination of a nose-down moment from ground effect and added power from the γ command lead to high-speed, nose-low touchdowns with the system engaged.

7) The most important system parameter, τ_1 (stick washout time constant), is optimum at about 2 seconds. This rate felt most natural with 1 second being too fast and 3 seconds too slow.

REFERENCES

1. Miller, G. K., Jr., Deal, P. L., and Champine, R. A.: Fixed Base Simulation Study of Decoupled Controls During Approach and Landing of a STOL Transport Airplane. NASA TN D-7363, February 1974.

2. Miller, G. K., Jr., and Deal, P. L.: Moving-Base Visual Simulation Study of Decoupled Controls During Approach and Landing of a STOL Transport Aircraft. NASA TN D-7790, January 1975.

3. Seckel, E. and Feinreich, B.: In-Flight Simulation Study of Decoupled Longitudinal Controls for the Approach and Landing of a STOL Aircraft. NASA TM X-73, 170, May 1976.

4. Ashkenas, I. L. and McReuer, D. T.: A Theory of Handling Qualities Derived from Pilot-Vehicle System Considerations. Institute of Aerospace Sciences Paper 62-39, 1962.

5. Stapleford, R. L. and Ashkenas, I. L.: Effects of Manual Attitude Control and Other Factors on Short-Period Handling Quality Requirements. AIAA Vol. 5, No. 1, Jan-Feb 1968.

6. Seckel, E.: The Landing Flare: An Analysis and Flight-Test Investigation. NASA CR-2517, 1975.

7. Shapira, J.: Classification of Longitudinal Controls. Princeton University Report AMS 1305-T, 1976.

8. Olcott, J. W., Seckel, E., and Ellis, D. R.: Analysis and Flight Evaluation of a Small, Fixed-Wing Aircraft Equipped with Hinged-Plate Spoilers. ARAP Report No. 233, 1977.

9. Sembongi, S.: Theoretical and Experimental Investigation of Flight Path Controllability and APC Concepts. Princeton University Report AMS 1294-T, 1976.

10. McRuer, D., Ashkenas, I. L., and Graham, D.: "Aircraft Dynamics and Automatic Control." Princeton University Press, 1973.

11. Franklin, J. A.: Turbulence and Longitudinal Flying Qualities. NASA CR-1821, July 1971.

12. Harper, R. P., Jr., and Cooper, G. E.: The Use of Pilot Rating in the Evaluation of Aircraft Handling Qualities. NASA TN D-5152, April 1969.

APPENDIX A

FORCE-FEEL STICK SYSTEM

General Operation

The key element in the system which was actually built and flown is a hydraulic servomechanism. Pilot input (stick force) is sensed by strain gages and this signal then becomes the input to the stick force model which electronically computes (analog computation) what the corresponding stick displacement should be. The output of the model is thus a commanded stick position and becomes the input to a stick positioner device (servo with position feedback). This appendix will show how the stick force equation was modeled.

Stick Force Equation Model

Essentially the forces felt by a pilot can be grouped in the following four types of forces:

- Forces due to aerodynamic hinge moments on the control surfaces.
- Forces due to mechanical-inertial properties of the stick, elevator and cable system.
- Bobweight and downspring forces.
- Servo actuator force feedbacks in the case of using a fully powered hydraulic system.

The following section will demonstrate how these forces can be simplified into a convenient form for simulation purposes.

Force-Feel Stick Model for In-Flight Simulator

Stick Force Due to Aerodynamic Hinge Moments - The stick force due to the aerodynamic hinge moment is simply

$$F_a = -GH \tag{A1}$$

where G is a constant representing the elevator stick gearing and H represents

the sum of all aerodynamic hinge moments.* Hinge moments may be nondimensionalized according to

$$H = 1/2\rho V^2 S_e c_e C_H \tag{A2}$$

or

$$H = q\, S_e c_e C_H \tag{A3}$$

S_e represents the surfaces area of the elevator and c_e is the elevator chord. C_H depends mainly on elevator deflection, angle of attack of the tail, and tab deflection. C_H also depends on elevator deflection rate or $\dot{\delta}_e$ as well as $\dot{\alpha}_t$, $\dot{\theta}$ and V, but for simplicity these effects were ignored. Therefore the stick force due to aerodynamic hinge moments may be represented by

$$F_a = - qS_e c_e G(C_{H\alpha}\alpha_t + C_{H\delta e}\cdot\delta_e + C_{H\delta_{tab}}\cdot\delta_{tab}) \tag{A4}$$

assuming a linear relation for the parameters $C_{H\alpha}$, $C_{H\delta e}$ and $C_{H\delta_{tab}}$. For simplicity assume that

$$K_a = - S_e c_e G(C_{H\alpha}\cdot\alpha_t + C_{H\delta e}\cdot\delta_e + C_{H\delta_{tab}}\cdot\delta_{tab}) \tag{A5}$$

This results in the following simplification

$$F_a = K_a \cdot q \tag{A6}$$

Stick Forces Due to the Mechanical-Inertial Properties of Control System - These forces can be expressed simply as the sum of three terms: inertia force, viscous friction force and Coulomb friction force.

$$F = I_{eff}\,\ddot{\delta}_s + B\dot{\delta}_s + F_c \tag{A7}$$

I_{eff} represents the effective control system moment of inertia; B is the viscous friction coefficient (constant). The last term, F_c, represents Coulomb friction and generally is:

$$F_c = C\,|\dot{\delta}_s|/\dot{\delta}_s \tag{A8}$$

*Seckel, E., "Stability and Control of Airplanes and Helicopters," Academic Press, April 1964.

Here C is the Coulomb friction magnitude.

Bobweight and Downspring Forces - The inadvertent mass unbalance in the control system of the airplane is considered a bobweight, since it has the same effect as a bobweight on the control system characteristics.

The force from the bobweight is expressed generally as

$$F_b = K_b \cdot n_z \tag{A9}$$

or

$$F_b = N_b(\alpha \text{ or } \delta_e) n_z \tag{A10}$$

Here K_b = linear bobweight constant

$N_b(\alpha \text{ or } \delta_e)$ = nonlinear coefficient when the nonlinear control system is employed

n_z = normal acceleration

The downspring force may be represented by the following equations:

$$\begin{aligned} F_d &= K_d \quad ; \text{ ordinary downspring (constant)} \\ &= N_d(\delta_s \text{ or } \alpha); \text{ nonlinear downspring (force depends on stick position or angle of attack)} \end{aligned} \tag{A11}$$

Servo Actuator Force Feedbacks - When fully powered control systems are employed there exist servo actuator force feedbacks such as a force due to hydraulic flow in the valve and valve force, etc.

These forces were neglected for simplicity and were not simulated in the control-feel system which was installed in the in-flight simulator.

Synthesis of Force-Feel System - From the above analysis, the stick force, which should be simulated in the force-feel system, can be expressed by the following equation

$$F_s = I_{eff} \ddot{\delta}_s + B \dot{\delta}_s + F_c + K_a \cdot q + K_b \cdot n_z + K_d \tag{A12}$$

where normal downsprings and bobweights are employed. The general expressions for the nonlinear downsprings and bobweights are:

$$F_b = N_b(\alpha \text{ or } \delta_e) \cdot n_z$$

and

$$F_d = N_d(\alpha \text{ or } \delta_e) \tag{A13}$$

The block diagram representation of this stick force model is shown in Figure A1.

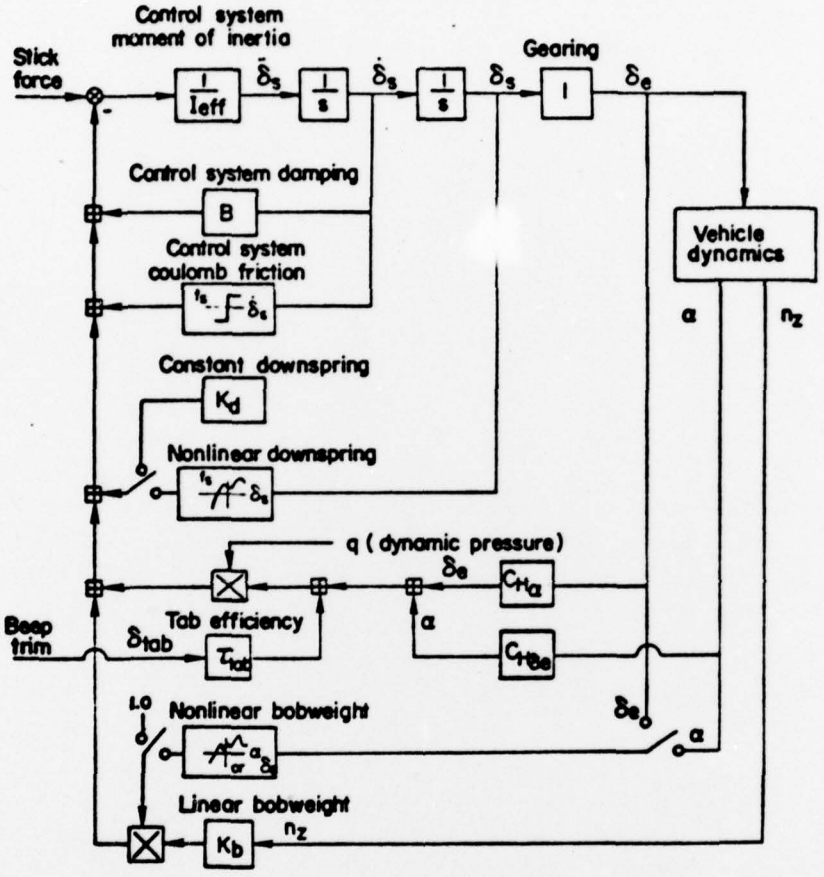

Figure A1. Block Diagram Representation of Force Feel Stick System.

Force-Feel Stick System for Fixed-Base Simulator

From the previous section the total stick force was shown to be:

$$F_s = I_{eff}\ddot{\delta}_s + B\dot{\delta}_s + F_c - \frac{1}{2}\rho V^2 S_e c_e G\,(C_{H\alpha}\cdot\alpha_t + C_{H_{\delta e}}\cdot\delta_e + C_{H_{\delta_{tab}}}\cdot\delta_{tab}) + F_b + F_d \qquad \text{(A14)}$$

Assume that the force due to the bobweight and downspring are from ordinary bobweights and downsprings. Therefore

$$F_b = K_b \cdot n_z \quad \text{and} \quad F_d = K_d \tag{A15}$$

We will also neglect the term $C_{H\alpha}$ since it is typically nearly equal to zero. Temporarily neglecting the Coulomb friction term results in

$$F_s = I_{eff}\ddot{\delta}_s + B\dot{\delta}_s + KV^2(C_{H\delta e}\cdot\delta_e + C_{H\delta_{tab}}\cdot\delta_{tab}) + K_b\cdot n_z + K_d \tag{A16}$$

where $$K = -\frac{1}{2}\rho S_e c_e G$$

To make the stick force equation suitable for an analog computer, it is convenient to linearize about an equilibrium condition. The stick force equation can then be expressed as follows

$$F_s = I_{eff}(\ddot{\delta}_{s_o} + \Delta\ddot{\delta}_s) + B(\dot{\delta}_{s_o} + \Delta\dot{\delta}_s) + K(V_o + \Delta V)^2\left[C_{H\delta e}(\delta_{e_o} + \Delta\delta_e) + C_{H\delta_{tab}}(\delta_{tab_o} + \Delta\delta_{tab})\right] + K_b\left[n_{z_o} + \Delta n_z\right] + K_d \tag{A17}$$

By neglecting second order terms such as $\Delta V^2\cdot\Delta\delta_e$ or $\Delta V\cdot\Delta\delta_e$ etc. the stick force equation becomes

$$F_s = I_{eff}(\ddot{\delta}_{s_o} + \Delta\ddot{\delta}_s) + B(\dot{\delta}_{s_o} + \Delta\delta_s) + KV_o^2\left[C_{H\delta e}\cdot\delta_{e_o} + C_{H\delta e}\cdot\Delta\delta_e + C_{H\delta_{tab}}\cdot\delta_{tab_o} + C_{H\delta_{tab}}\cdot\Delta\delta_{tab}\right] + 2KV_o\Delta V\left[C_{H\delta e}\cdot\delta_{e_o} + C_{H\delta_{tab}}\cdot\delta_{tab_o}\right] + K_b\left[n_{z_o} + \Delta n_z\right] + K_d \tag{A18}$$

Since the initial condition was one of trim flight, $\ddot{\delta}_{s_o}$ and $\dot{\delta}_s$ will both be zero. Also for trim flight the following condition must be true

$$K_b(n_{z_o}) + K_d = KV_o^2\left[C_{H\delta e}\cdot\delta_{e_o} + C_{H\delta_{tab}}\cdot\delta_{tab_o}\right] \tag{A19}$$

This simply says that <u>initially</u> any force due to downspring and bobweight must be balanced by the sum of the initial aerodynamic hinge moments. Therefore the stick force equation now becomes

$$F_s = I_{eff}\ddot{\Delta\delta}_s + B\dot{\Delta\delta}_s + KV_o^2\left[C_{H\delta e}\cdot\Delta\delta_e + C_{H\delta_{tab}}\cdot\Delta\delta_{tab}\right]$$

$$+ 2KV_o\Delta V\left[C_{H\delta e}\cdot\delta_{e_o} + C_{H\delta_{tab}}\cdot\delta_{tab_o}\right] + K_b(\Delta n_z) \qquad \text{(A20)}$$

The term

$$2KV_o\Delta V\left[C_{H\delta e}\cdot\delta_{e_o} + C_{H\delta_{tab}}\cdot\delta_{tab_o}\right] = \frac{2\cdot\Delta V\cdot V_o^2K}{V_o}\left[C_{H\delta e}\cdot\delta_{e_o} + C_{H\delta_{tab}}\cdot\delta_{tab_o}\right]$$

but

$$V_o^2K\left[C_{H\delta e}\cdot\delta_{e_o} + C_{H\delta_{tab}}\cdot\delta_{tab_o}\right] = F_d + F_b$$

Therefore

$$F_s = I_{eff}\ddot{\Delta\delta}_s + B\dot{\Delta\delta}_s + G(H_{\delta e}\cdot\Delta\delta_e + H_{\delta_{tab}}\cdot\Delta\delta_{tab})$$

$$+ K_b(\Delta n_z) + 2(F_d+F_b)\Delta V/V_o \qquad \text{(A21)}$$

The equation is almost in a form suitable for simulation purposes. Since $G\cdot\Delta\delta_e = \Delta\delta_s$ the equation becomes:

$$F_s = I_{eff}\ddot{\Delta\delta}_e + B\dot{\Delta\delta}_s + H_{\delta e}\cdot\Delta\delta_s + GH_{\delta tab}\cdot\Delta\delta_{tab}$$

$$+ K_b(\Delta n_z) + 2(F_d+F_b)\Delta V/V_o \qquad \text{(A22)}$$

or

$$\left[F_s - GH_{\delta tab}\cdot\Delta\delta_{tab} - K_b(\Delta n_z) - 2(F_d+F_b)\Delta V/V_o\right] 1/H_{\delta e} =$$

$$I_{eff}\ddot{\Delta\delta}_s/H_{\delta e} + (B/H_{\delta e})\dot{\Delta\delta}_s + \Delta\delta_s$$

$$\left[F_s - GH_{\delta tab}\cdot\Delta\delta_{tab} - K_b(\Delta n_z) - 2(F_d+F_b)\Delta V/V_o\right] 1/H_{\delta e} =$$

$$\ddot{\Delta\delta}_s/\omega^2 + 2\zeta\dot{\Delta\delta}_s/\omega + \Delta\delta_s \qquad \text{(A23)}$$

where $\omega^2 = H_{\delta e}/I_{eff}$ and $2\zeta\omega = B/I_{eff}$

The above equation essentially represents the stick force equation as it might be modeled for simulation purposes. The right hand side is a simple second order differential equation and may be represented as shown in Figure A2.

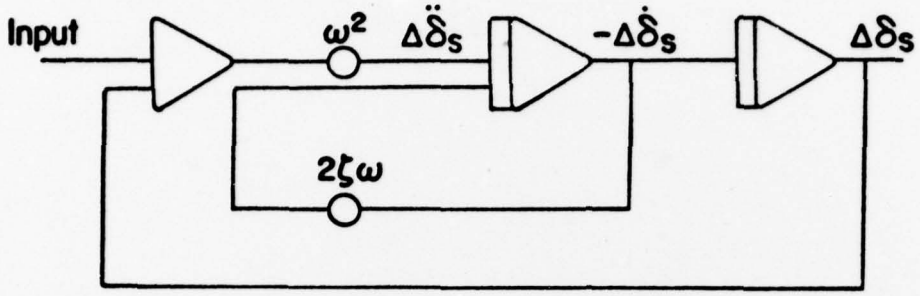

Figure A2. Second Order Stick-Force Model.

Temporarily, assuming no input, the model is simply a representation of

$$\Delta\ddot{\delta}_s/\omega^2 + 2\zeta\Delta\dot{\delta}_s/\omega + \Delta\delta_s = 0 \qquad \text{(A24)}$$

or

$$\Delta\ddot{\delta}_s/\omega^2 = (-2\zeta/\omega)\ \Delta\dot{\delta}_s - \Delta\delta_s \qquad \text{(A25)}$$

multiplying by both sides by ω^2

$$\Delta\ddot{\delta}_s = -2\zeta\omega\Delta\dot{\delta}_s - \Delta\delta_s\omega^2 \qquad \text{(A26)}$$

exactly the representation shown above.

For simplification the model tested used only a force input and other inputs such as tab, n_z, downspring and bobweights were neglected. This gives

$$F_s = \Delta\ddot{\delta}_s/\omega^2 + 2\zeta\Delta\dot{\delta}_s/\omega + \Delta\delta_s \qquad \text{(A27)}$$

and this is shown in Figure A3.

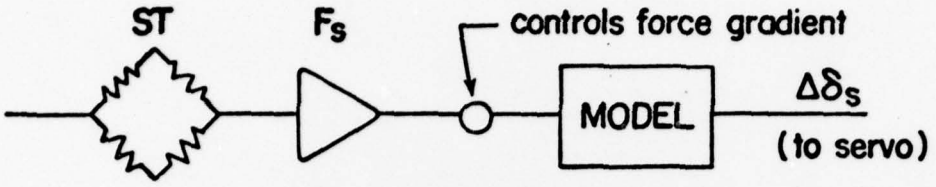

Figure A3. Block Diagram Representation of Analog Computer System.

The potentiometer shown represents the force gradient and may be varied to give different levels.

APPENDIX B

PILOT OPINION RATING SCALE

Pilot rating were based on the revised Cooper-Harper scale described in Reference 12 and also shown below.

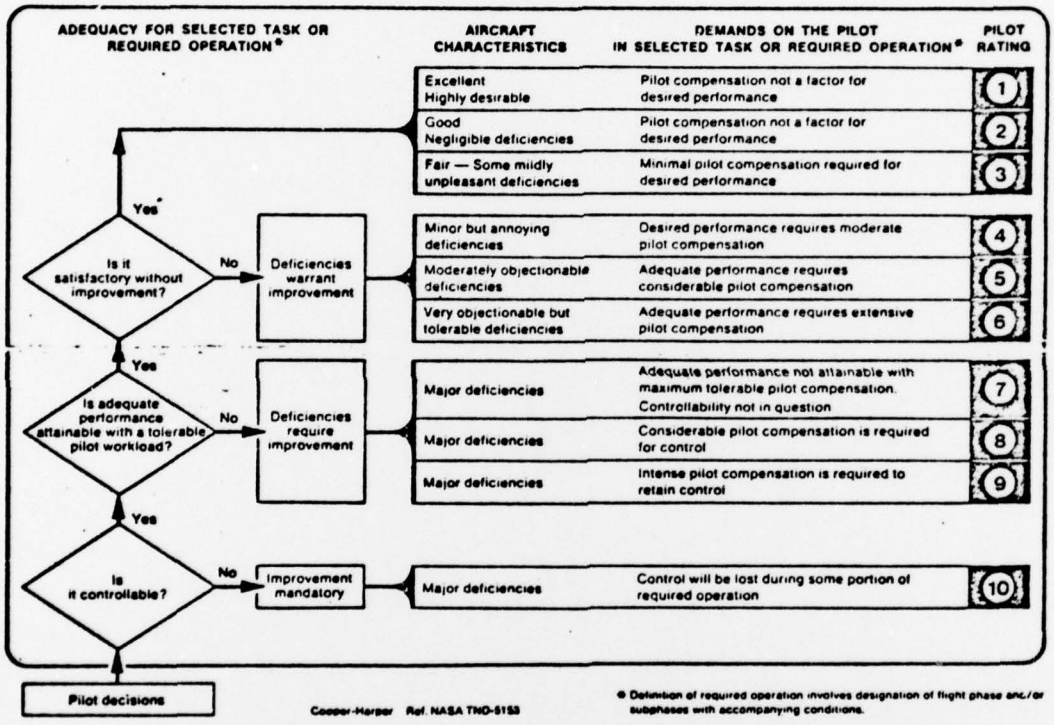

Figure B1. The Cooper-Harper Pilot Rating Scale.

APPENDIX C

STABILITY DERIVATIVES OF BASIC NAVION

The longitudinal stability derivatives of the basic Navion at 70 kt which were employed for the fixed base simulations and analytical studies are listed as follows:

$D_v - T_v$	0.16	1/sec
$D_\alpha - g$	-12.0	m/rad sec^2
L_v/V	0.00491	1/m
L_α/V	1.2	1/sec
M_v	0	rad/m sec
M_α	-6.1	$1/sec^2$
$M_{\dot{\alpha}}$	-0.82	1/sec
$M_{\dot{\theta}}$	-1.7	1/sec
$M_{\delta e}$	-8.7	$1/sec^2$
$T_{\delta t}$	0.081	$m/sec^2/\%$

APPENDIX D

NOTATION

B	viscous friction coefficient, newton-sec/m
C	coulomb friction magnitude, newton
$C_{H\alpha}$	nondimensional angle of attack hinge moment coefficient, floating tendency
$C_{H_{\delta e}}$	nondimensional elevator deflection hinge moment coefficient, restoring tendency
$C_{H\delta_{tab}}$	nondimensional tab hinge moment coefficient
C_L	nondimensional lift coefficient
c_e	chord of elevator, m
D_v	drag due to velocity = 1/m ($\partial D/\partial V$), 1/sec
D_α	drag due to angle of attack = 1/m ($\partial D/\partial \alpha$), m/rad sec^2
F_a	aerodynamic stick force, newton
F_c	stick force due to coulomb friction, newton
F_d	stick force due to downspring, newton
F_s	stick force, newton
G	stick to elevator gearing constant, rad/m
g	acceleration due to gravity, 9.81 m/sec^2
H	elevator hinge moment, newton-m
$H_{\delta e}$	dimensional hinge moment due to elevator deflection, newton-m
$H_{\delta t}$	dimensional hinge moment due to tab deflection, newton-m
h	altitude, m
h_c	command altitude, m
IFR	instrument flight rules
I_{eff}	effective moment of inertia of control system, kg-m^2
I_Y	pitch moment of inertia, kg-m^2
K	$-1/2\ \rho\ S_e c_e$
K_a	$-S_e c_e G(C_{H\alpha} \cdot \alpha_t + C_{H\delta e} \cdot \delta_e + C_{H\delta_{tab}} \cdot \delta_{tab})$
K_b	linear bobweight constant
K_{ph}	altitude control loop pilot gain
K_{pv}	velocity control loop pilot gain
$K_{p\theta}$	pitch attitude control loop pilot gain

K_{servo}	servo gain
L_v/V	lift due to velocity = $1/mV\ (\partial L/\partial V)$, 1/m
L_α/V	lift due to angle of attack = $1/mV\ (\partial L/\partial \alpha)$, 1/sec
M_v	pitching moment due to velocity = $1/I_Y\ (\partial M/\partial V)$, rad/m sec
M_α	pitching moment due to angle of attack = $1/I_Y\ (\partial M/\partial \alpha)$, $1/sec^2$
$M_{\delta e}$	pitching moment due to elevator deflection = $1/I_Y\ (\partial M/\partial \delta e)$, $1/sec^2$
$M_{\delta t}$	pitching moment due to throttle deflection = $1/I_Y\ (\partial M/\partial \delta t)$, rad/sec^2 per unit δ_t
$M_{\dot{\theta}}$	pitch damping = $1/I_Y\ (\partial M/\partial \dot{\theta})$, 1/sec
m	airplane mass, kg
mac	mean aerodynamic chord
n_b	nonlinear bobweight constant
n_z	normal acceleration, m/sec^2
p_g	rolling moment gust, rad/sec
q	dynamic pressure, $newton/m^2$
S_e	surface area of elevator, m^2
S_T	stick to throttle crossfeed gain
s	Laplace operator, 1/sec
T_s	throttle to stick (elevator) crossfeed gain
$T_{\delta t}$	thrust due to throttle deflection = $1/m\ (\partial T/\partial_{\delta t})$ m/sec^2 per unit δ_t
u_g	horizontal velocity gust, m/sec
V	velocity, m/sec, knot
VFR	visual flight rules
w_g	vertical velocity gust, m/sec
α	angle of attack, deg, rad
α_g	angle of attack gust, deg, rad
α_t	angle of attack of tail, deg, rad
γ	flight path angle
Δ	longitudinal characteristic equation
δ_e	elevator deflection, deg, rad
δ_s	stick deflection, m
δ_t	throttle deflection, %
δ_{tab}	tab deflection, deg, rad